学位論文（要約）

Study on the functions of BES1 family transcription factors in differentiation of vascular stem cells in *Arabidopsis thaliana*

（シロイヌナズナの維管束幹細胞分化における BES1 転写因子ファミリーの機能解析）

平成 29 年 12 月博士（理学）申請

東京大学大学院理学系研究科

生物科学専攻

齊藤　真人

Contents

Acknowledgements

I would like to express my sincerest appreciation to Prof. Hiroo Fukuda for giving me opportunity to study in his laboratory and supervision and encouragement throughout this study. I wish to express my deepest gratitude to Dr. Mitsutomo Abe, Prof. Hiroyuki Hirano, Prof. Hirokazu Tsukaya and Dr. Kyoko Ohashi-Ito for their reviews and critical comments on this thesis. I would like to offer my special thanks to Dr. Yuki Kondo for continuous support and valuable advice. I would like to acknowledge Dr. Takeshi Nakano, Dr. Holger Puchta, Dr. Shigeo Sugano and Dr. Michael Knoblauch for providing materials. I also thank Dr. Kuninori Iwamoto, Dr. Satoshi Endo, Dr. Shigeyuki Betsuyaku, Dr. Chieko Saito, Dr. Satoshi Naramoto, Ms. Yasuko Ozawa, Ms. Yukiko Sugisawa for technical support. I am grateful to all other Prof. Fukuda lab members.

List of Abbreviations

2,4-D	2,4-dichlorophenoxy acetic acid
ABRC	Arabidopsis Biological Resource Center
ACT2	ACTIN 2
APL	ALTERED PHLOEM DEVELOPMENT
ARF	AUXIN RESPONSE FACTOR
ARR	ARABIDOPSIS RESPONSE REGULATOR
ATHB8	ARABIDOPSIS THALIANA HOMEOBOX GENE 8
BEH	BES1/BZR1 HOMOLOG
BES1	BRI1-EMS-SUPPRESSOR 1
BiFC	bimolecular fluorescence complementation
BL	brassinolide
BR	brassinosteroid
BRAVO	BRASSINOSTEROIDS AT VASCULAR AND ORGANIZING CENTER
BRI1	BRASSINOSTEROID-INSENSITIVE 1
BRRE	BR response element
BZR1	BRASSINAZOLE RESISTANT 1
Cas9	CRISPR-associated 9
cDNA	complementary DNA
CDS	coding sequence
CRISPR	clustered regularly interspaced short palindromic repeats
CVP2	COTYLEDON VASCULAR PATTERN 2
cYFP	C-terminal yellow fluorescent protein
DMSO	dimethyl sulfoxide
EAR	ethylene-responsive element binding factor-associated amphiphilic repression
EGL3	ENHANCER OF GLABRA 3
gBES1	genomic BES1
GO	gene-ontology

GSK3	glycogen synthase kinase 3 protein
GUS	β-glucuronidase
HA	hemagglutinin
HD-ZIP	homeodomain-leucin zipper
IRX3	IRREGULAR XYLEM 3
LBD	LATERAL ORGAN BOUNDARIES
LHCB2.1	LIGHT-HARVESTING CHLOROPHYLL B-BINDING 2.1
MS	Murashige and Skoog
NAC	NAM, ATAF1/2 and CUC2
NLS	nuclear localization signal
nYFP	N-terminal yellow fluorescent protein
PCR	polymerase chain reaction
PI	propidium iodide
PP2A	protein phosphatase 2A
QC	quiescent center
qRT-PCR	quantitative reverse transcription PCR
RbcS3B	RUBISCO SMALL SUBUNIT 3B
RNAi	RNA interference
SAUR-AC1	Arabidopsis Columbia SMALL AUXIN UP RNA gene 1
SEOR1	SIEVE-ELEMENT-OCCLUSION-RELATED 1
sGFP	synthetic green fluorescent protein
SK	GSK3/SHAGGY-like kinase
SMXL5	SUPPRESSOR OF MAX2 1-LIKE5
SRDX	superman repression domain ver. X
T-DNA	transfer DNA
TDIF	tracheary element differentiation inhibitory factor
TDR	TDIF RECEPTOR
TTG1	TRANSPARENT TESTA GLABRA 1
TUB2	TUBULIN BETA CHAIN 2
UBQ14	UBIQUITIN 14
VISUAL	Vascular cell Induction culture System Using Arabidopsis Leaves

VND	VASCULAR-RELATED NAC-DOMAIN
VP	VISUAL phloem specific gene
WT	wild type
XCP1	XYLEM CYSTEINE PEPTIDASE 1

Abstract

Vascular development is an excellent model for studying cell differentiation in plants. Two conductive tissues, the xylem and phloem, are derived from common stem cells known as procambial/cambial cells. Recent studies have revealed that glycogen synthase kinase 3 proteins (GSK3s), downstream of the tracheary element differentiation inhibitory factor (TDIF)-TDIF receptor (TDR) signal, play crucial roles in maintaining procambial/cambial cells by suppressing their differentiation into xylem or phloem cells. However, it remains to be uncovered how GSK3s regulate differentiation from procambial cell.

Recently, an *in vitro* culture system for analyzing vascular cell differentiation named VISUAL (Vascular cell Induction culture System Using Arabidopsis Leaves) has been established (Kondo et al., 2016), which is suitable for elucidating the above-mentioned question. In this thesis, therefore, I tried to indicate the downstream signaling of GSK3s using VISUAL.

First, I searched transcription factors downstream of GSK3s. In Chapter III-1, I show that the transcription factor BRI1-EMS-SUPPRESSOR 1 (BES1) is a major downstream target of GSK3s in xylem differentiation by searching known GSK3s substrates. I indicated that *bes1* mutants exhibited xylem differentiation defects in VISUAL and that introduction of *BES1* completely complemented mutant phenotypes.

Secondly, I investigated whether phloem differentiation is also regulated by GSK3s. In Chapter III-2 and III-3, I show that BES1 promotes not only xylem but also phloem cell differentiation from procambial cells. Transcriptome analysis of the *bes1* mutants during culture in VISUAL revealed that phloem-related genes were

downregulated in *bes1* mutants similar to the mutant of *ALTERED PHLOEM DEVELOPMENT* (*APL*), which is a key regulator of the initiation of phloem differentiation. This result suggests that BES1 regulates the early process of phloem differentiation.

該当部分に関して、
5 年以内に雑誌で刊行予定のため、非公開。

In conclusion, I found that BES1 family transcription factors are key regulators of xylem and phloem differentiation from procambial cells downstream of GSK3s.

該当部分に関して、5 年以内に雑誌で刊行予定のため、非公開。

該当部分に関して、5 年以内に雑誌で刊行予定のため、非公開。

Chapter I: Introduction

Vascular tissues, consisting of xylem and phloem cells, are required for long-distance transport of various materials in plants. The xylem transports water and minerals from roots to shoots, whereas, in most cases, the phloem transports photoassimilates from shoots to roots. Although xylem and phloem cells have different structures and functions, these cells originate from common stem cells known as procambial/cambial cells. Previous studies identified master regulators of xylem and phloem cell fate. VASCULAR-RELATED NAC-DOMAINs (VNDs) facilitate xylem differentiation (Kubo et al., 2005), whereas ALTERED PHLOEM DEVELOPMENT (APL) is required for phloem development (Bonke et al., 2003). Molecular analyses of these master regulators have revealed the downstream components controlling various developmental events associated with xylem and phloem differentiation (Ohashi-Ito et al., 2010; Yamaguchi et al., 2011; Furuta et al., 2014b). Prior to the final determination of cell fate, glycogen synthase kinase 3 proteins (GSK3s) regulate vascular cell differentiation as earlier regulators (Kondo et al., 2014). GSK3s are activated by perception of a phloem-derived peptide, tracheary element differentiation inhibitory factor (TDIF), by TDIF receptor (TDR) at plasma membrane (Ito et al., 2006; Hirakawa et al., 2008). Then the SKI and SKII subgroups of GSK3s redundantly maintain procambial cell populations by suppressing xylem differentiation. Indeed, the application of the GSK3s inhibitor bikinin (De Rybel et al., 2009) induces ectopic xylem cell differentiation in the presence of auxin and cytokinin (Kondo et al., 2014, 2015). Based on this finding, Kondo et al. (2016) established a powerful tissue culture system for xylem cell differentiation named VISUAL (Vascular cell Induction culture System Using

Arabidopsis Leaves). In VISUAL, phloem cells are also differentiated from procambial cells depending on bikinin treatment (Kondo et al., 2016), indicating that GSK3s can control also phloem differentiation. However, it remains to be elucidated how GSK3s regulate both of xylem and phloem differentiation.

GSK3s in plants are first identified in the brassinosteroid (BR) signaling pathway. In the absence of BR, GSK3s directly phosphorylate BRI1-EMS-SUPRESSOR 1 (BES1) family transcription factors. Phosphorylated BES1 family is transferred from nucleus to cytosol by 14-3-3 proteins and then degraded by proteasome (He et al., 2002; Gampala et al., 2007; Ryu et al., 2007, 2010). Once BRs are perceived by a cell surface receptor BRASSINOSTEROID-INSENSITIVE 1 (BRI1), GSK3s are inactivated (Li et al., 2002) and then BES1 family members are activated via dephosphorylation by protein phosphatase 2A (PP2A) to control downstream gene expression (Tang et al., 2011). BES1 family can control the thousands of genes as both of transcriptional activators and repressors (He et al., 2005; Sun et al., 2010; Yu et al., 2011). Previous studies suggest that BR promotes xylem differentiation (Yamamoto et al., 1997; Choe et al., 1999; Nagata et al., 2001), raising the possibility that BES1 family is the target of GSK3s in xylem differentiation.

Arabidopsis contains six members of the BES1 family. Among these, BES1 and its closest homolog, BRASSINAZOLE RESISTANT 1 (BZR1), are considered to be major mediators of BR signaling. However, our understanding of the BR signaling pathway has primarily been obtained from studies using the gain-of-function mutants *bes1-D* and *bzr1-D* (Yin et al., 2002; Wang et al., 2002). By contrast, few loss-of-function studies investigating BES1 family members have been performed (Yin et al., 2005). In particular, loss-of-function mutants for *BZR1* have not yet been reported.

Therefore, our understanding of the contribution of BES1 and BZR1 to BR signaling remains incomplete. Recent advances in genome editing techniques, including CRISPR/Cas9 (clustered regularly interspaced short palindromic repeats/CRISPR-associated 9) system, should allow the actual functions of genes of interest to be analyzed by generating knock-out mutants.

該当部分に関して、5 年以内に雑誌で刊行予定のため、非公開。

In this study, I investigated the functions of BES1 family members in vascular cell differentiation using loss-of-function mutants. I newly established *bzr1* mutants by the CRISPR/Cas9 system. VISUAL experiments using obtained mutants uncovered that BES1 is a main player of vascular cell differentiation. Comprehensive gene expression analysis of the *bes1* mutants revealed that BES1 positively regulates both xylem and phloem differentiation, but not procambial cell differentiation from mesophyll cells, in VISUAL. Further genetic analysis with *bes1 bzr1* mutants indicated that BES1 and BZR1 act redundantly in promoting both xylem and phloem differentiation. Interestingly, the phenotypes when cultured in VISUAL were weaker in *bzr1* than in *bes1*, indicating that BES1 and BZR1 contribute differently to vascular development. On the other hand, observation of *in vivo* vasculature of *bes1 bzr1* and comparison of *bes1 bzr1* with BR-deficient mutants suggest the further functional redundancy of BES1 family members.

該当部分に関して、5 年以内に雑誌で刊行予定のため、非公開。

Altogether, my results suggest that vascular differentiation from procambial cells is regulated through the balance of activation and inhibition by BES1 family members.

Chapter II: Materials and Methods

Plant materials

Seeds of the *Arabidopsis thaliana bes1-1* (SALK_098634), *bes1-2* (WiscDsLox246D02), *bes1-3* (SALK_091133)

該当部分に関して、5 年以内に雑誌で刊行予定のため、非公開。

were obtained from the Arabidopsis Biological Resource Center (ABRC).

該当部分に関して、5 年以内に雑誌で刊行予定のため、非公開。

The progeny of heterozygous *bri1-48* (SALK_041648) were gifts from Dr. Takeshi Nakano (RIKEN, Japan), and homozygous mutants were identified based on the presence of severely shortened hypocotyls. *bes1-D* and *bzr1-D* mutants were also gifts from Dr. Takeshi Nakano and *bes1-D bzr1-D* mutants were generated by crossing. *pSEOR1::SEOR1-YFP* seeds was given by Dr. Michael Knoblauch (Washington State University, USA). All mutants in this study were the Columbia background. To produce the complementation lines, genomic DNA fragments of *BES1* containing the 2k-bp promoter sequence and the 1k-bp sequence downstream of the stop codon were cloned and introduced into the pGWB1 vector (Nakagawa et al., 2007).

該当部分に関して、5 年以内に雑誌で刊行予定のため、非公開。

該当部分に関して、5 年以内に雑誌で刊行予定のため、非公開。

Transformation of WT and *bes1-1* plants was performed by the floral dip method (Clough and Bent, 1998). Plants were grown on conventional 1/2 Murashige and Skoog (MS) agar plates (pH 5.7) at 22°C under continuous light unless otherwise mentioned. For later harvesting, seedlings were transferred to pots containing a mixture of vermiculite (VS Kakou) and PRO-MIX BX (Premier Horticulture).

CRISPR

The target sequence was selected using CRISPRdirect software (Naito et al., 2015). DNA fragments containing 20 bp of the target sequence neighboring the PAM sequence and overhang sequences were generated by hybridizing two primers, followed by ligation into the pEn-Chimera vector (Fauser et al., 2014) that had been digested with *Bbs*I. The sgRNA-containing sequence was then transferred into the pDe-CAS9 vector (Fauser et al., 2014) via LR reaction (Thermo Fisher Scientific). The resulting construct was transformed into WT and *bes1-1* plants. Transformants were obtained by bialaphos selection. T2 seeds from single insertion lines were incubated on MS agar plates without antibiotics. *Cas9*-free mutants were selected from the T2 population by PCR and sequencing using the primers listed in Table 2. To check the sequence of *BZR1* transcript in *bes1-1 bzr1-2*, total RNA was extracted from cotyledons of 6-day-old WT and *bes1-1 bzr1-2* plants using an RNeasy Plant Mini kit (Qiagen). Reverse transcription was performed using SuperScript III (Thermo Fisher Scientific). PCR was performed using synthesized cDNA and the primers listed in Table 2, followed by

sequencing using the same primer. Data were visualized using Chromas 2.6 (http://technelysium.com.au/wp/).

VISUAL

The previously described protocol was used (Kondo et al., 2016). In brief, cotyledons of 6-day-old seedlings grown in liquid 1/2 MS medium were cultured in MS-based medium containing 0.25 mg/l 2,4-D, 1.25 mg/l kinetin, and 10 μM bikinin under continuous light. To compare the phenotypes of *bes1-1* vs. *bes1-1 bzr1-2*, the bikinin concentration was changed to 20 μM. To observe ectopic xylem differentiation, cotyledons cultured for 4 days were fixed in ethanol/acetic acid (3:1, v/v) and mounted with clearing solution (chloral hydrate/glycerol/water; 8:1:2, w/w/v). The differentiation rates were determined based on the area of ectopic xylem cells in a cotyledon per total area of the cotyledon blade. These areas were calculated using ImageJ.

RT-PCR

該当部分に関して、5 年以内に雑誌で刊行予定のため、非公開。

qRT-PCR

Total RNA was extracted from cotyledons before or after culture for 72 h (in the VISUAL experiments) or from whole seedlings treated with DMSO or 100 μM BL for 3

h (in the BL sensitivity tests) using an RNeasy Plant Mini kit (Qiagen). Quantitative PCR was performed using a LightCycler (Roche Diagnostics). Mesophyll, procambium, xylem and phloem marker genes were selected by following references: Sawchuk et al., 2008; Endo et al., 2014; Kondo et al., 2015. *UBQ14* was used for the VISUAL experiments, and *ACTIN 2* (*ACT2*) was used for the BL sensitivity tests as an internal control. The gene-specific primer sets are listed in Table 2.

Microarray experiment

Microarray analyses were performed as previously described (Ohashi-Ito et al., 2010). For clustering, normalization of gene expression levels was performed as follows: First, the average fold-change between values before and after induction in each experiment was calculated. These values were then normalized by dividing them by the median value of the WT, *bes1-3*, and *bes1-1*. Finally, these values were converted to log2 scale, producing a value defined as the Processed signal. Hierarchical clustering via the Pearson correlation method and heatmap generation were performed using Subio Platform software (Subio). The half-time point was defined as the first time point when the relative expression level reached 50% of its maximum value in a set of time-course microarray data (Kondo et al., 2015) in which the expression levels between observed values were postulated to change linearly. GO enrichment analysis was performed using DAVID Bioinformatics Resources 6.8 (Huang et al., 2009; https://david.ncifcrf.gov/). Phloem specific genes in roots were selected by S32 (phloem marker)-specific expression levels (> 2-fold compared to any other markers) in deposited microarray data (Brady et al., 2007).

Histological analysis

Hypocotyls of 11-day- or 16-day-old plants grown in liquid 1/2 MS medium were fixed in FAA (40% (v/v) ethanol, 2.5% (v/v) acetic acid, 2.5% (v/v) formalin) and gradually dehydrated by ethanol series. Samples were embedded in Technovit 7100 resin (Kulzer). Sections at 5 μm thickness were produced by using a RM2165 microtome (Leica). Sliced samples were stained with 0.1% (w/v) toluidine blue for 1 min. To produce cross-sections of 6-week-old plants, hypocotyls or the basal parts of stems were fixed in 70% (v/v) ethanol. Sections of hypocotyls and stems 2 cm above the rosette at 80 μm thickness were produced using a LEICA VT1200S vibratome. Sliced samples were stained with 0.05% (w/v) aniline blue in 100 mM phosphate buffer (pH 7.2) for 1 h and observed under UV irradiation.

BR treatment

To observe hypocotyl or root elongation, plants were grown on 1/2 MS agar plates containing DMSO or BL. After 7 days, the plates were scanned with a CanoScan 9000F (Canon). Hypocotyl and root length were measured using ImageJ. For gene expression analysis, plants were grown on 1/2 MS agar plates. After 10 days, the seedlings were incubated in a solution of DMSO or 100 μM BL for 3 h and collected for RNA extraction.

Phenotypic observation of dark-grown plants

Plants were grown on 1/2 MS agar plates in the dark after white light irradiation to promote germination. After 7 days, the plates were scanned using a CanoScan 9000F (Canon). Hypocotyl length was measured using ImageJ.

Statistical analysis

For multiple comparisons, Tamhane T2 tests were employed in this study due to inhomogeneous variances obtained by the Levene tests (Wallner et al., 2017). The significance thresholds were set to $\alpha = 0.05$. The *p*-values for each comparison were calculated by Welch's t-test. The significance threshold of each comparison was set to $\alpha'=1-(1-\alpha)^{1/k}$, where k is the total number of comparisons. For example, if $k = 3$, the significance threshold of the *p*-value of each comparison (α') is approximately 0.0167.

Comparison of amino acid sequences among BES1 family

Amino acid sequences of BES1 family were obtained from The Arabidopsis Information Resource (TAIR) website (https://www.arabidopsis.org/). Only BEH2 was manually corrected because the registered sequence did not match that of cDNA, which was consistent with Verhoef et al. (2013). An Alignment of amino acid sequences of BES1 family and generation of a phylogenetic tree with neighbor-joining method was performed by ClustalX ver. 2.1 (http://www.clustal.org/).

Observation of BES1 expression

GFP fluorescence of *gBES1-sGFP/bes1-1* cultured in VISUAL for 2 days was observed by fluorescent microscope (BX51, Olympus). To observe hypocotyl, 18-day-old *gBES1-sGFP/bes1-1* hypocotyls were fixed with 4% (w/v) PFA in PBS for 1 h. Sections of hypocotyls at 150 μm thickness were produced using a LEICA VT1200S vibratome. To observe roots, 7-day-old *gBES1-sGFP/bes1-1* roots were briefly stained with 20 μg/ml solution of propidium iodide (PI) (Thermo Fisher Scientific) and washed with

water. Fluorescence was observed using confocal laser scanning microscope (FV1200, Olympus).

Transient expression in *Nicotiana benthamiana*

For promoter-reporter assay, DNA fragments 2-kb upstream of the translation initiation codon of *SAUR-AC1* were cloned into pENTR/D-TOPO vector (Thermo Fisher Scientific) and transferred into the pGWB434 vector (Nakagawa et al., 2007) via LR reaction (Thermo Fisher Scientific).

該当部分に関して、5 年以内に雑誌で刊行予定のため、非公開。

Rhizobium radiobacter GV3101 MP90 strain harboring these constructs was infiltrated into *Nicotiana benthamiana* leaves with the strain harboring a construct of p19k suppressor. For GUS-staining, leaves were cut and treated with 10 μM estrogen (and 10 μM bikinin). Then samples were fixed with 90% (v/v) acetone overnight at -20°C. After washed with 100 mM sodium phosphate buffer (pH 7.0), leaves were stained in GUS staining solution [1 mg/ml 5-bromo-4-chloro-3-indolyl glucuronide, 2.5 mM potassium ferricyanide, 2.5 mM potassium ferrocyanide, 100 mM sodium

phosphate buffer (pH 7.0)] overnight at 37°C. After rinsed with 70% (v/v) ethanol, samples were transferred into ethanol/acetic acid (3:1, v/v) and mounted with clearing solution. In BiFC assay, fluorescence in leaves were observed at 3 days after infiltration using fluorescent microscope (BX51, Olympus).

Chapter III: Results

III-1: BES1 positively regulates xylem cell differentiation in VISUAL

To identify transcription factors downstream of GSK3s in vascular development, I tried to observe mutant phenotypes of known targets of GSK3s. Although GSK3s regulate several transcription factors, I first focused on BES1/BZR1 family, which are considered as key GSK3s targets in BR signaling pathway (Wang et al., 2002; Yin et al., 2002; Yin et al., 2005). In this study, I used an *in vitro* culture system named VISUAL (Kondo et al., 2016; Fig. 1) to evaluate the vascular cell differentiation without considering the effect of cell proliferation.

該当部分に関して、5 年以内に雑誌で刊行予定のため、非公開。

GSK3s directly phosphorylate BES1/BZR1 family and then BES1/BZR1 are inactivated and degraded by proteasome (He et al., 2002). Because inhibition of GSK3s activities promotes xylem differentiation, it was hypothesized that the loss of BES1/BZR1 family proteins may prevent xylem differentiation.

該当部分に関して、5 年以内に雑誌で刊行予定のため、非公開。

Because no T-DNA insertion line for *BZR1* was available, CRISPR/Cas9 system (Fauser et al., 2014) was employed to generate *bzr1* knock-out mutants. I successfully generated plants that possess a 1 base insertion in the second exon of *BZR1* and the *Cas9* gene had been removed (Fig. 4A). This insertion resulted in the appearance of a premature stop codon due to a frameshift (Fig. 4B), thus the mutant was named *bzr1-1*.

該当部分に関して、5 年以内に雑誌で刊行予定のため、非公開。

To test whether BES1 family members are involved in xylem differentiation, ectopic xylem differentiation in these mutants was examined by VISUAL.

該当部分に関して、5 年以内に雑誌で刊行予定のため、非公開。

This result suggests that BES1 is the most important member regulating xylem differentiation downstream of GSK3s in the BES1/BZR1 family.

To further confirm the role of BES1 in vascular development, I obtained three T-DNA insertion lines for *BES1*: *bes1-1* (He et al., 2005), *bes1-2* (Lachowiec et al., 2013), and *bes1-3* (previously named *bes1-2* in Kang et al., 2015, and *bes1* in Kondo et al., 2014) (Fig. 3). The cotyledons of these mutants commonly exhibited reduced xylem differentiation at 96 h after VISUAL induction (Fig. 6). Differentiation rates in *bes1-1* and *bes1-2* mutants were lower than that in *bes1-3*, indicating that *bes1-1* and *bes1-2* are strong alleles and that *bes1-3* is a weak allele. Next, I introduced a genomic fragment of *BES1* (*gBES1*) into *bes1-1* for complementation assay. The introduction completely restored the reduced ectopic xylem differentiation rate in *bes1-1* (Fig. 7). These results indicate that BES1 is responsible gene for xylem differentiation defect of *bes1* T-DNA insertion mutants.

III-2: BES1 promotes xylem cell differentiation from procambial cells in VISUAL

In VISUAL, mesophyll cells first differentiate into procambial cells, followed by xylem cells (Kondo et al., 2015; Fig. 1). I therefore examined whether procambial cells are

normally induced in *bes1* or not. First, I performed detailed phenotypic analysis of *bes1-3* (weak allele) and *bes1-1* (strong allele) by measuring the expression levels of procambium and xylem marker genes. RNA samples were collected at 72 h after induction, when xylem-related genes were expressed at maximum levels. qRT-PCR analysis indicated that the expression levels of xylem marker genes such as *IRREGULAR XYLEM 3* (*IRX3*) and *XYLEM CYSTEINE PEPTIDASE 1* (*XCP1*) were lower in the *bes1* mutants than in the WT (Fig. 8A, B). Consistent with the observation of ectopic xylem, expression levels of xylem-related genes were lower in *bes1-1* than in *bes1-3*. By contrast, the procambium-specific gene *TDR* was not downregulated in *bes1* mutants in VISUAL (Fig. 8C). This result suggests that procambial formation is not inhibited in *bes1*. Thus, I hypothesized that BES1 specifically promotes xylem differentiation from procambial cells.

Next, to comprehensively identify downstream and upstream factors for BES1, I performed microarray analysis of cotyledons at 72 h after VISUAL induction in *bes1-1*, *bes1-3*, and the WT. I initially selected genes that were highly upregulated at 72 h after VISUAL induction in the WT (>4-fold upregulation, 1534 genes; Kondo et al., 2016) as vascular-related genes. Hierarchical clustering classified the vascular-related genes into two major groups (Fig. 9A). Approximately 60% of the vascular-related genes were downregulated in *bes1* mutants. Then I designated these genes as a "*bes1*-down" group (Fig. 9A). On the other hand, nearly 40% of vascular-related genes were expressed at the same or higher level in the mutants. Therefore, I categorized these genes as a "*bes1*-not-down" group (Fig. 9A). To characterize these two groups of genes, I analyzed the expression profiles of the *bes1*-down group and the *bes1*-not-down group using previously reported time-course microarray data from leaf disks cultured in VISUAL

(Kondo et al., 2015). Most *bes1*-down genes showed maximum expression at 60 h after induction, whereas many *bes1*-not-down genes were induced at 36 h after induction (Fig. 9B). Further half-time point analysis, which evaluates the timing of gene expression in VISUAL, indicated that the expression of the *bes1*-not-down genes increased from 12 to 26 h and that of the *bes1*-down genes increased from 30 to 48 h in VISUAL (Fig. 9C). These results indicate that, in the *bes1* mutants, the late stage of VISUAL is suppressed, whereas the early stage is not suppressed but is instead promoted.

I then conducted gene-ontology (GO) enrichment analysis to characterize the molecular functions of the *bes1*-down and *bes1*-not-down genes. In the *bes1*-down group, secondary cell wall-related genes, including xylan and lignin biosynthesis genes, were markedly enriched (Table 1). Additionally, genes related to xylem vessel cell differentiation were also enriched in this group (Table 1). These results coincide with the finding that *bes1* mutants show defects in xylem differentiation in VISUAL. On the other hand, procambial cell-related genes were enriched in the *bes1*-not-down group (Table 1). Moreover, the *bes1*-not-down group contained many genes related to cell cycle and cell division (Table 1) including seven out of eight previously identified procambial-specific genes that were upregulated in VISUAL only in the presence of bikinin (Kondo et al., 2015). Some *bes1*-not-down genes were annotated as auxin-related genes, which seem to be implicated in procambium formation in leaves (Furuta et al., 2014a). These results suggest that, in cultured *bes1* cotyledons, procambial cells accumulate due to the inhibition of differentiation of procambial cells into xylem cells. Altogether, these data support my hypothesis that BES1 promotes xylem cell differentiation from procambial cells in VISUAL.

該当部分に関して、5 年以内に雑誌で刊行予定のため、非公開。

該当部分に関して、5 年以内に雑誌で刊行予定のため、非公開。

III-3: BES1 also promotes phloem cell differentiation in VISUAL

In VISUAL, phloem sieve element-like cells also differentiate from procambial cells (Kondo et al., 2016). Interestingly, several *bes1*-down genes were annotated as being related to phloem development (Table 1). Consistent with this notion, qRT-PCR analysis indicated that the expression levels of phloem marker genes *APL* and *SIEVE-ELEMENT-OCCLUSION-RELATED 1* (*SEOR1*) were significantly reduced in the *bes1* mutants compared with the WT, which is similar to xylem marker genes (Fig. 11A, B). These results suggest that phloem differentiation is also suppressed in *bes1*. The introduction of *gBES1* into *bes1-1* fully complemented reduced expression of phloem marker genes as well as that of xylem marker genes in *bes1-1* (Fig. 12A). These results strongly support the idea that BES1 promotes phloem differentiation as well as xylem differentiation (Fig. 12B).

To understand the role of BES1 in phloem development, I investigated *bes1*-related expression of “VISUAL phloem-specific genes” (VPs; Fig. 11C), which were identified by transcriptome data in VISUAL (Kondo et al., 2016) and in roots (Brady et al., 2007), using microarray. Many VPs were downregulated in the *bes1*

mutants (Fig. 11D). In phloem development, APL is known as a master regulator (Bonke et al., 2003) and *apl* mutants have strong defects only in phloem development in VISUAL (Kondo et al., 2016). I found that most of VPs were commonly downregulated in *bes1-1* and *apl* mutants (Fig. 11E). Considering the significant reduction in *APL* expression in *bes1-1* (Fig. 11A), these data suggest that BES1 upregulates a wide range of phloem sieve element-related genes, likely upstream of APL.

III-4:

この章に関して、5 年以内に雑誌で刊行予定のため、非公開。

III-5:

この章に関して、5 年以内に雑誌で刊行予定のため、非公開。

III-6: BZR1 acts redundantly with BES1 in vascular development

In *bes1* mutants, the induction of both xylem and phloem marker genes in VISUAL was not completely repressed, suggesting that other factors may contribute to the promotion of the differentiation process. BZR1 is the closest homolog of BES1, with 88% identity (Wang et al., 2002) and *bzr1* mutants showed partial reduction of xylem differentiation in VISUAL (Fig. 5C). Therefore I tried to generate *bes1 bzr1* double mutants. By using a CRISPR/Cas9 system, (Fauser et al., 2014) in *bes1-1*, I succeeded in obtaining a homozygous line which has lost 29 bases of *BZR1* spanning from the 3' end of the intron to the start of the second exon (Fig. 18A) and the *Cas9* gene had been removed. Sequencing of *BZR1* transcripts revealed that the splicing site between the intron and the second exon is altered in this line (Fig. 18B), leading to a premature stop codon due to a frameshift (Fig. 18C). Hereafter this line is named *bes1-1 bzr1-2*.

I tried to examine redundant and different roles of BES1 and BZR1 in vascular cell differentiation using *bes1-1 bzr1-2* double mutants. However, the *bes1-1* mutants produced relatively small amounts of xylem cells under the original VISUAL conditions, making it difficult to verify the functional redundancy of *BES1* and *BZR1*. Then, I increased the bikinin concentration in the culture medium to 20 μM in order to induce more xylem cells in the background of *bes1-1* (Fig. 19A, B, D), which allowed me to detect the effect of *bzr1*. Under this condition, the xylem differentiation rate was much lower in the *bes1-1 bzr1-2* mutants than in *bes1-1* (Fig. 19B, C, D). The downregulation

of xylem and phloem marker genes in the *bes1* single mutants was also enhanced by the addition of the *bzr1-2* mutation (Fig. 19E). On the other hand, the procambium marker gene *TDR* was not repressed even in *bes1-1 bzr1-2* (Fig. 19E). Based on these results, it is likely that BZR1 acts redundantly with BES1 in xylem and phloem differentiation from procambial cells in VISUAL.

The *bzr1-1* single mutants showed slightly reduced xylem differentiation rates (Fig. 20A-D) and xylem marker gene expression, when compared with the WT (Fig. 20E). The expression levels of phloem marker genes were not significantly different from those of the WT ($p = 0.136$ for *APL* and $p = 0.036$ for *SEOR1*), but they tended to be reduced in *bzr1-1* (Fig. 20E). Thus, the mutant phenotypes of *bzr1-1* were weaker than those of *bes1-1* in terms of differentiation rate and xylem and phloem gene expression levels when cultured in VISUAL. These results suggest that BZR1 is also involved in xylem and phloem differentiation, but to a lesser extent than BES1.

III-7: *BES1* and *BZR1* gain-of-function mutations promote differentiation from procambial cells *in vivo*

Next I examined whether BES1 and BZR1 regulate vascular differentiation *in planta*. For this purpose, I used gain-of-function mutants *bes1-D* and *bzr1-D*, which stabilize BES1 or BZR1, respectively (Li et al., 2002; Yin et al., 2002), and generated *bes1-D bzr1-D* double gain-of-function mutants. Overall morphology of *bes1-D bzr1-D* was similar to that of *bes1-D*, in which hypocotyl is elongated (Yin et al., 2002) but thickness of hypocotyl is comparable with the WT. In WT hypocotyls, usually two or three procambial cell layers were formed between phloem and xylem cells (Fig. 21A). In *bes1-D bzr1-D*, however, procambial cell layers were reduced, occasionally resulting

in adjacency of xylem and phloem cells (Fig. 21B; Red arrowhead). In addition, ectopic phloem cells, which are non-clustered phloem cells surrounded by undifferentiated cells, were sometimes formed only in *bes1-D bzr1-D* but not in WT (Fig. 21C; Yellow arrowhead). These results suggest that BES1 and BZR1 promote the differentiation from procambial cells *in vivo*.

III-8: Growth defects are not observed in *bes1-1 bzr1-2* mutants

To investigate whether BES1 and BZR1 are essential for *in vivo* vascular development, I compared cross-sections from WT vs. *bes1-1 bzr1-2* plants. Although *bes1-1 bzr1-2* mutants showed severe defects in VISUAL, no obvious defect was observed in the central xylem tissues of hypocotyls in 16-day-old or 6-week-old plants (Fig. 22A-D). Phloem tissues (visualized by toluidine blue and aniline blue staining) were also indistinguishable between the WT and *bes1-1 bzr1-2* (Fig. 22C, D). Similarly, no defects in vascular development were observed in 6-week-old stems of *bes1-1 bzr1-2* (Fig. 22E, F). These results suggest that the vascular phenotype of *bes1-1 bzr1-2* is enhanced in the culture system VISUAL, in which exogenous bikinin induces rapid vascular cell differentiation apart from other developmental processes.

BES1 and BZR1 are involved in various developmental processes. In particular, they function as major transcription factors that mediate the BR signaling pathway (Guo et al., 2013). To explore the impact of BES1 and BZR1 on BR signaling, I treated WT and *bes1-1 bzr1-2* plants with a bioactive BR, brassinolide (BL). BL treatment promotes hypocotyl elongation and represses root growth in WT plants in the light (Fig. 23A, B). As previously reported (He et al., 2005; Kang et al., 2015), *bes1-1* was slightly resistant to exogenous BL (Fig. 23A, B). Although *bzr1-1* single mutants were partially resistant

to exogenous BL only in root elongation (Fig. 23B), the *bes1-1 bzr1-2* mutants were more insensitive to BL than the *bes1* single mutants in terms of both hypocotyl and root elongation (Fig. 23A, B). Consistent with this observation, the changes in expression of a BR-responsive gene in response to BL treatment were also partially reduced in *bes1-1 bzr1-2* (Fig. 24). Next, I examined defects related to BR signaling in *bes1-1 bzr1-2* in the absence of exogenous BL treatment. The *bri1* mutant, a BR receptor mutant, shows severe defects in hypocotyl elongation under dark conditions (Li and Chory, 1997). However, *bes1-1* and *bes1-1 bzr1-2* did not exhibit such a phenotype, instead appearing like WT plants (Fig. 23C, D). Furthermore, stem growth in *bes1-1 bzr1-2* was comparable to that in the WT under normal growth conditions (Fig. 25), unlike the dwarf mutant *bri1*. Thus, the BR-related phenotype in *bes1-1 bzr1-2* was observed only in the presence of exogenously applied BL.

III-9:

この章に関して、5 年以内に雑誌で刊行予定のため、非公開。

Chapter IV: Discussion

BES1 promotes xylem and phloem differentiation from procambial cells but not procambial cell differentiation from mesophyll cell

Previously, it was reported that GSK3s maintain procambial cells by inhibiting their differentiation (Kondo et al., 2014). In the current study, I found that *bes1* mutants have defects in xylem differentiation in an *in vitro* culture system named VISUAL (Kondo et al., 2016). *bes1-1* is a strong allele, but this mutant likely expresses a splice variant *BES1-S*. BES1-L has additional N-terminal NLS and is proposed to have stronger function than BES1-S (Jiang et al., 2015). Therefore, it could be possible that BES1-L functions in vascular development predominantly.

In VISUAL, mesophyll cells initially differentiate into procambial cells, followed by xylem or phloem cells (Kondo et al., 2015, 2016). Bikinin promotes procambial cell differentiation (Kondo et al., 2015) as well as the differentiation of procambial cells into xylem and phloem cells (Kondo et al., 2016). However, microarray analysis with *bes1* mutants showed that BES1 does not affect procambial cell formation from mesophyll cell. Therefore, it is likely that GSK3s also control procambial cell differentiation, but factors other than BES1 are involved in this process downstream of the GSK3s. Indeed, GSK3s phosphorylate various developmental regulators such as ENHANCER OF GLABRA 3 (EGL3) and TRANSPARENT TESTA GLABRA 1 (TTG1) (Cheng et al., 2014) for root hair formation and AUXIN RESPONSE FACTOR 7 (ARF7) and ARF19 for lateral root formation (Cho et al., 2014). Therefore, it will be interesting to identify a new target(s) of GSK3s that regulates procambial cell differentiation.

I also found that BES1 plays a positive role in phloem differentiation as well as xylem differentiation. Gene expression analyses indicate that BES1 positively regulates phloem differentiation upstream of the master transcription factor APL. Similarly, the xylem master gene *VND7* was also activated downstream of BES1. Therefore, it is likely that BES1 functions early in vascular development before the induction of final differentiation by master regulators of xylem and phloem differentiation. These findings, together with the observation that a large number of procambial cells remained in the *bes1* mutants after the induction of VISUAL, suggest that BES1 triggers the transition of stem cells to specialized cells into xylem or phloem cells.

該当部分に関して、5 年以内に雑誌で刊行予定のため、非公開。

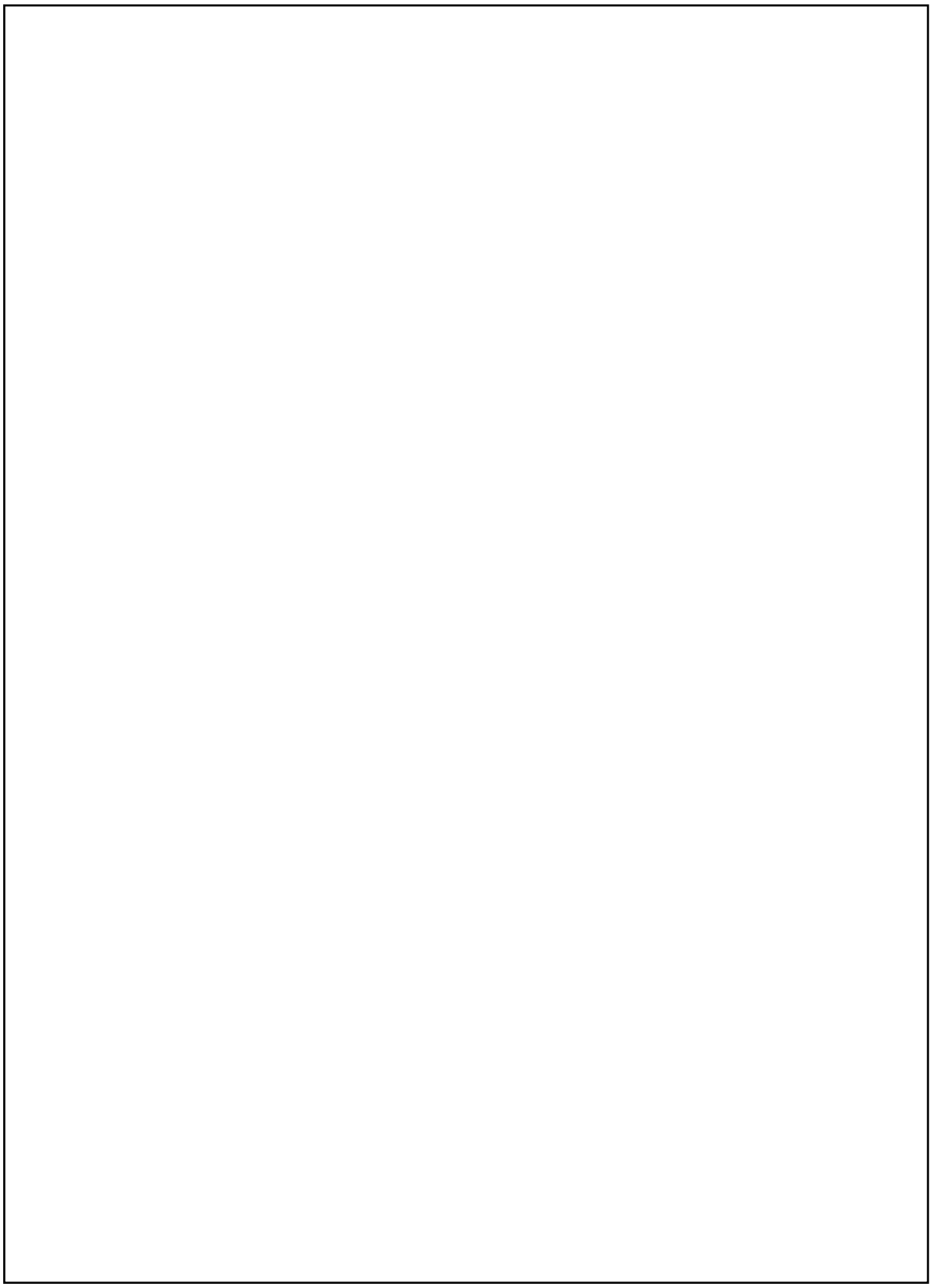

Differential contribution of BES1 and BZR1 to vascular cell differentiation

VISUAL using *bzr1-1* and *bes1-1 bzr1-2* revealed that BZR1 as well as BES1 positively regulates both xylem and phloem differentiation from procambial cells. This finding is consistent with the previous finding that both *bes1-D* and *bzr1-D* can partially rescue the phenotype of *octopus* mutant, in which root protophloem differentiation is prone to be repressed (Anne et al., 2015). My observation that phloem cells are ectopically produced in hypocotyls of *bes1-D bzr1-D* also supports the molecular functions of BES1 and BZR1 found in VISUAL. In the current study, *bes1* exhibited a stronger vascular phenotype than *bzr1-1*, and the phenotype induced by these mutations was additive, suggesting that BES1 and BZR1 redundantly function in xylem and phloem differentiation to a greater and lesser extent, respectively. This is not self-evident because morphologies of *bes1-D* and *bzr1-D* are different under light condition, meaning that BES1 and BZR1 have somehow different functions. For example, *bzr1-D* mutants show BR-deficient phenotype due to strong negative feedback regulation of BR biosynthesis, whereas *bes1-D* show constitutive BR-active phenotypes (Wang et al., 2002; Yin et al., 2002).

該当部分に関して、5 年以内に雑誌で刊行予定のため、非公開。

Functional redundancy among BES1 family members

There are six *BES1*-like genes in the Arabidopsis genome: *BES1*, *BZR1*, and *BES1/BZR1 HOMOLOG 1–4* (*BEH1–4*) (Yin et al., 2002; Wang et al., 2002; Yin et al.,

2005). BES1 and BZR1 are thought to act as central players that regulate various developmental processes in plants, playing prominent roles in BR signaling (Guo et al., 2013). However, in many cases, functional analyses of these proteins have been performed using gain-of-function mutants (*bes1-D* and *bzr1-D*), and few analyses have been performed using loss-of-function mutants. Here, I produced *bzr1-1* and the *bes1-1 bzr1-2* double mutant to analyze the roles of BES1 and BZR1. The *bes1*, *bzr1-1*, and *bes1-1 bzr1-2* mutants did not show any visible phenotypes *in planta*, including a dwarf phenotype and photomorphogenesis in the dark, which are characteristic phenotypes of BR-deficient mutants such as *bri1*. This result strongly suggests that BES1 family members function redundantly. I then examined the phenotypes of these mutants in physiological aspects. The only mutant phenotype observed in *bes1-1 bzr1-2* was reduced sensitivity to exogenous BL application. To account for this phenomenon, the following findings about other multiple mutants should be considered. The *arabidopsis response regulator 10* (*arr10*) *arr12* double mutants are resistant to exogenous cytokinin but grow well on MS agar plates and in soil (Yokoyama et al., 2007). The addition of the *arr1* mutation to *arr10 arr12* results in plants with a dwarf phenotype in the absence of cytokinin, which was also observed in another cytokinin dominant-negative mutant, *wooden leg* (Yokoyama et al., 2007). Consistent with this idea, *bes1*-RNAi lines, which exhibit repressed expression not only of *BES1* and *BZR1* (Yin et al., 2005), but also of several *BEHs* (Wang et al., 2013), show defects in stem growth and shoot branching.

該当部分に関して、5 年以内に雑誌で刊行予定のため、非公開。

該当部分に関して、5 年以内に雑誌で刊行予定のため、非公開。

該当部分に関して、5 年以内に雑誌で刊行予定のため、非公開。

該当部分に関して、5 年以内に雑誌で刊行予定のため、非公開。

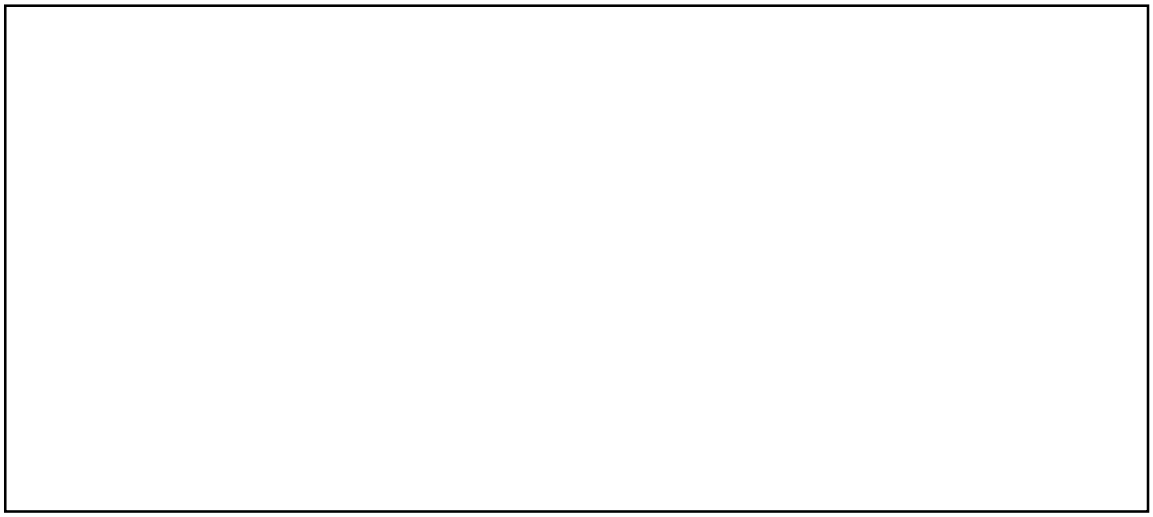

Table 1. GO enrichment analysis of vascular-related genes.

***bes1*-down genes**

Term	P-Value	Fold Enrichment
regulation of secondary cell wall biogenesis	2.07E-15	24.88
plant-type secondary cell wall biogenesis	1.29E-14	12.53
xylan biosynthetic process	5.44E-13	15.88
carbohydrate metabolic process	2.06E-07	2.75
glucuronoxylan biosynthetic process	9.15E-07	17.87
xylem development	1.56E-06	10.21
xylan metabolic process	4.09E-06	20.42
cell wall organization	4.79E-06	2.731
lignin catabolic process	1.55E-05	11.91
lignin biosynthetic process	6.65E-05	4.954
xylem vessel member cell differentiation	7.05E-05	19.14
cell wall thickening	1.35E-04	30.63
phloem development	6.40E-04	20.42
positive regulation of secondary cell wall biogenesis	6.40E-04	20.42

***bes1*-not-down genes**

Term	P-Value	Fold Enrichment
microtubule-based movement	2.19E-19	15.32
cell division	1.16E-14	6.134
response to auxin	3.22E-12	4.77
auxin-activated signaling pathway	3.10E-10	5.40
cell cycle	1.40E-08	6.211
mitotic nuclear division	4.34E-08	7.429
regulation of cell cycle	1.15E-07	7.625
multicellular organism development	6.54E-06	2.902
procambium histogenesis	2.85E-05	24.76
auxin polar transport	2.41E-04	6.368
cotyledon vascular tissue pattern formation	5.90E-04	12.38

GO enrichment analysis of genes upregulated in VISUAL (>4-fold, 1534 genes). The *bes1*-down and *bes1*-not-down groups were examined separately. Significantly enriched terms ($p < 0.001$) are shown.

Table 2. Lists of primers used in this study.

Cloning

該当部分に関して、5 年以内に雑誌で刊行予定のため、非公開。

RT-PCR

該当部分に関して、5 年以内に雑誌で刊行予定のため、非公開。

CRISPR

Name	Sequence	Object
BZR1-CRIS-sense	ATTGCCAGCTATCTCACCAGGTAA	Construction
BZR1-CRIS-antisense	AAACTTACCTGGTGAGATAGCTGG	Construction
SS42	TCCCAGGATTAGAATGATTAGG	Genotyping (*Cas9*) (http://www.botanik.kit.edu/molbio/940.php)
SS43	CGACTAAGGGTTTCTTATATGC	Genotyping (*Cas9*) (http://www.botanik.kit.edu/molbio/940.php)
BZR1-CR-geno_F	CGTCGACATCAGCATCTG	Genotyping (*BZR1*)
BZR1-CR-geno_R	GGGTATGAAACTGGTGGC	Genotyping/Sequencing (*BZR1*)

qRT-PCR

Gene	Left	Right	Probe
APL	TGGATATTCAGCGCAACGTA	TGCACTTCCATTTGCATCTC	#143
UBQ14	TCCGGATCAGCAGAGGTT	TCTGGATGTTGTAGTCAGCAAGA	#121
IRX3	TGACATGAATGGTGACGTAGC	CATCAAATGCTCCTTATCACCTT	#25
XCP1	TCCACAAAGAAGATGATTACCCTTA	TCACACGTTCCACATCCTCTT	#69
SEOR1	AAGACACCAACGCCTCCA	CGATAGCATAGGAGACACTATCAAGA	#136
LHCB2.1	CAAGTCTACTCCTCAAAGCATCTG	CGGTTAGGTAGGACGGTGTATT	#93
RbcS3B	ATCACTTCCATCGCAAGCA	AGAGTCTCAAACTTCTTCTTTCCAA	#103
TDR	ATTCAAACCGACGAATCCAT	TTCTGGTGCAATGTAACCGTA	#141
ATHB8	CTCAAGAGATTTCACAACCTAACG	TCACTGCTTCGTTGAATCCTT	#60
LBD15	AACGTCTCCAAGATGCTAATGG	AGGCTATTCGCGGCATCT	#106
ACT2	CCGCTCTTTCTTTCCAAGC	CCGGTACCATTGTCACACAC	#30
SAUR-AC1	AGGATTCATGGCGGTCTATG	GTATGAAACCGGCACCACAT	#143
VND1	GGAAAACACTTGTGTTCTACAAAGG	CAAACCACCCATCCTTCTTC	#137

VND2	CGAACCATGGGATTTACAAGA	TGTTTGTTCTTGTTCC	#5
VND3	CGAACCATGGGATCTACAAGA	CGGTTTGTCCTAGTCCCAGTC	#41
VND7	CACGAATACCGTCTCCAAAACT	CCTAAATGCTCGACACACCA	#69

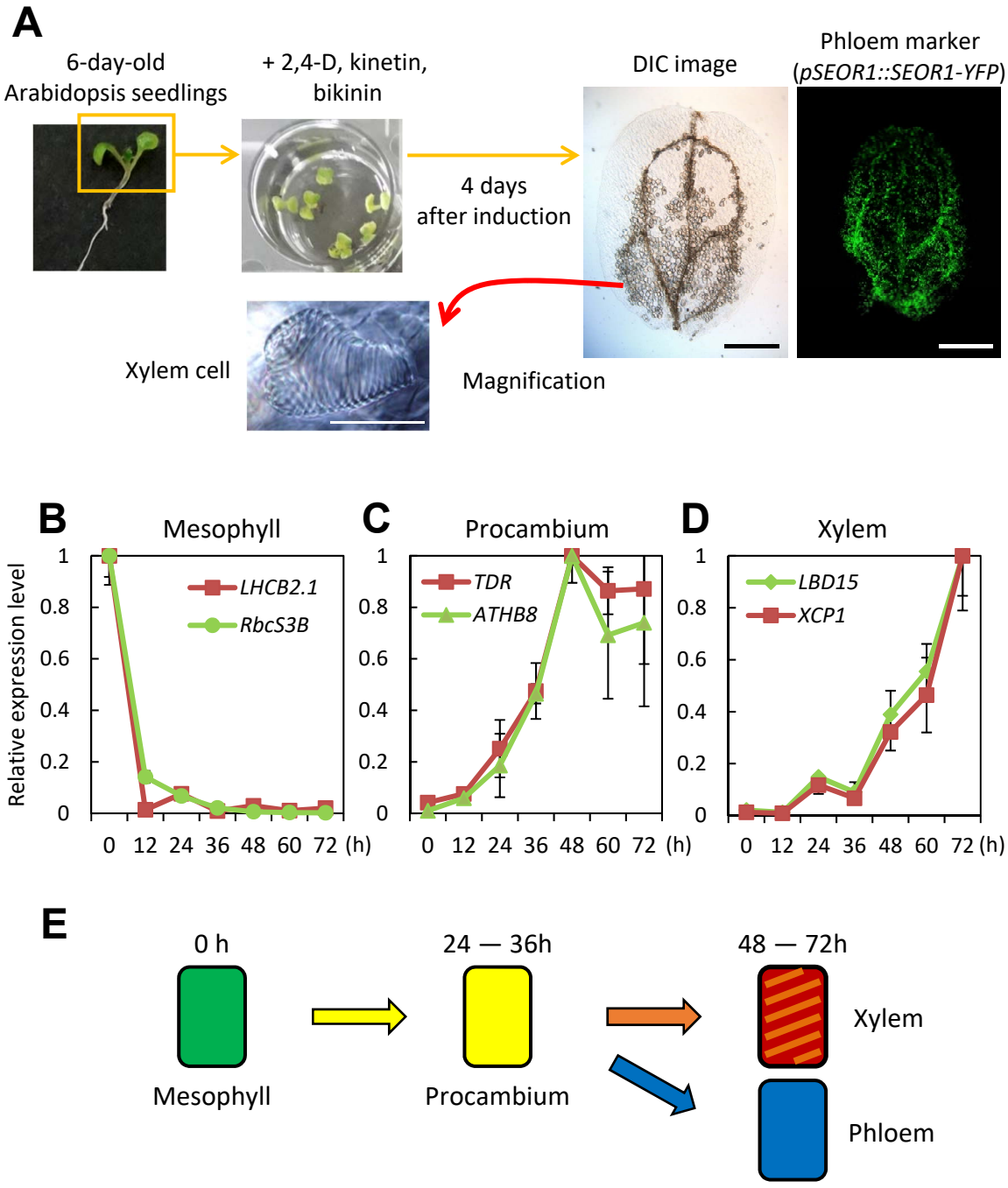

Figure 1. Overview of VISUAL using cotyledons

(A) A summary of VISUAL methods (Kondo et al., 2016). Cotyledons of 6-day-old Arabidopsis seedlings are cultured with auxin, cytokinin and GSK3-inhibitor named bikinin. After 4 days, ectopic xylem and phloem cells are observed. Scale bars indicate 1 mm (whole cotyledons) or 50 μm (magnification). (B-D) qRT-PCR analysis examining expression levels of mesophyll (B), procambium (C), xylem (D) marker genes every 12 h after induction. The maximum expression level of each gene is set to 1. Error bars indicate SD (n = 3). (E) Schematic illustrations of differentiation process in VISUAL.

5年以内に雑誌で刊行予定のため、非公開

Figure 2.

5年以内に雑誌で刊行予定のため、非公開

Figure 3.

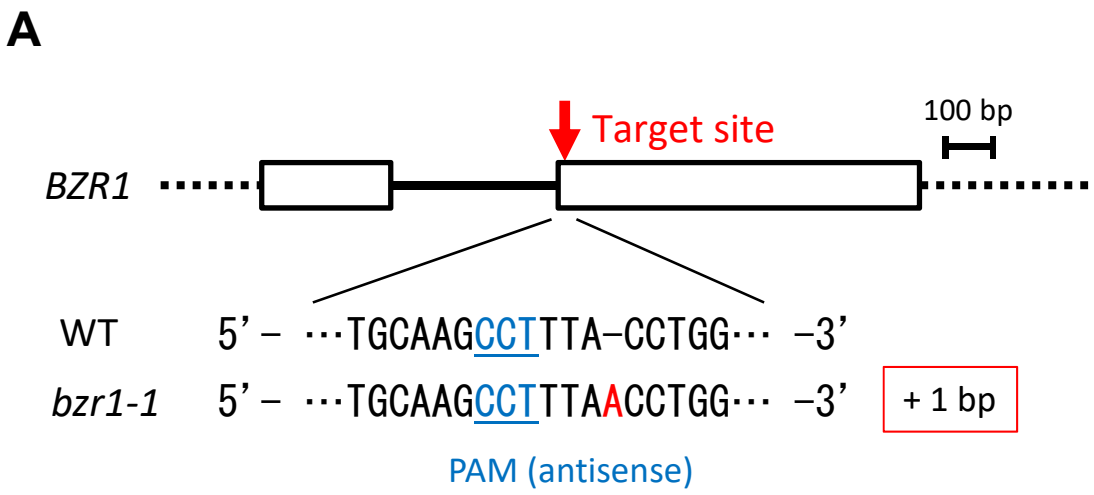

Figure 4. Generation of *bzr1* mutants.

(A) Schematic overview of the gene structure of *BZR1* and the sequence around the selected site targeted by CRISPR/Cas9. Exons, the intron, and UTRs are illustrated by boxes, a solid line, and dotted lines, respectively. Exon sequences in the WT are shown in uppercase letters. PAM sequences of the target and the resulting mutations are highlighted in blue and red, respectively. One base insertion was detected in *bzr1-1*. (B) Theoretical amino acid sequences of BZR1 around the mutated sites in the WT and *bzr1-1*. Asterisk represents premature stop codon.

5年以内に雑誌で刊行予定のため、非公開

Figure 5.

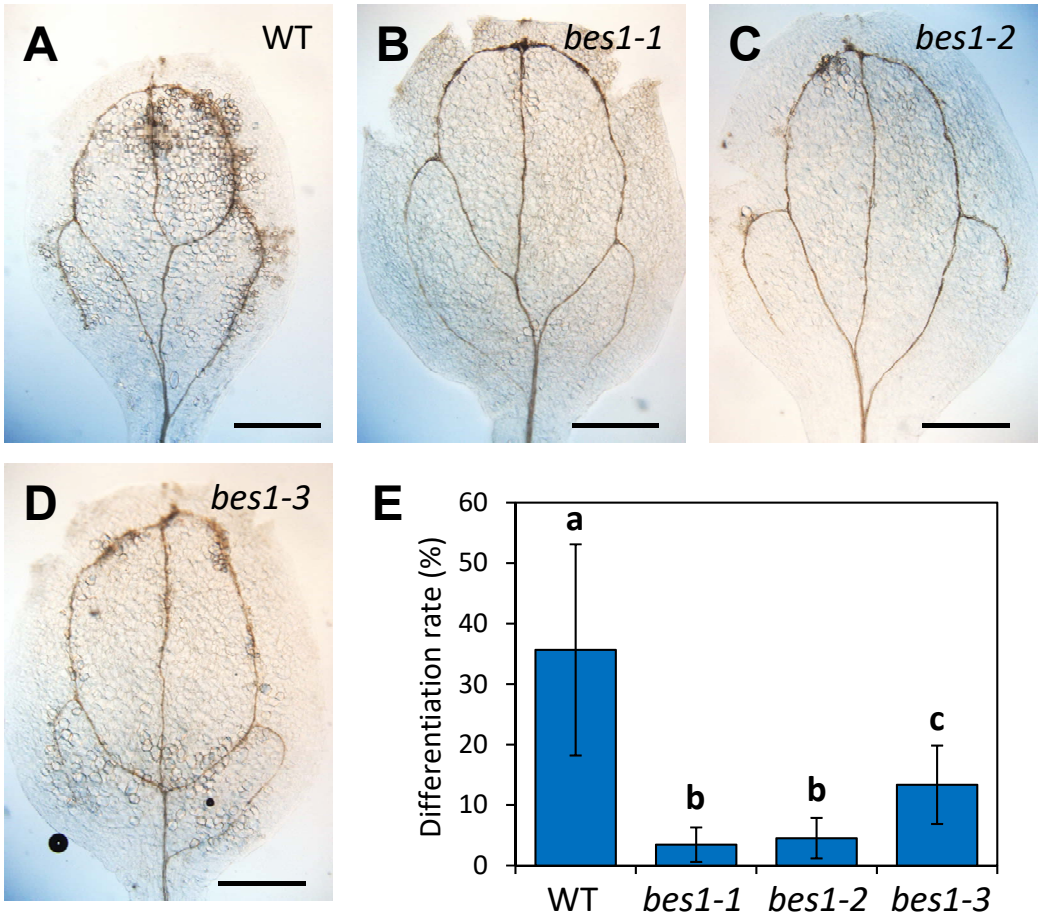

Figure 6. Xylem differentiation of *bes1* T-DNA insertion mutants in VISUAL.

(A-D) Ectopic xylem cell formation in VISUAL. WT (A), *bes1-1* (SALK_098634) (B), *bes1-2* (WiscDsLox246D02) (C), and *bes1-3* (SALK_091133) (D) cotyledons were cultured in medium containing 2,4-D, kinetin, and bikinin for 4 days. Scale bars indicate 1 mm. (E) Quantification of xylem differentiation rates in A-D. Error bars indicate SD (n = 8–10). Significant differences are indicated by different letters (Tamhane T2 test, $\alpha = 0.05$).

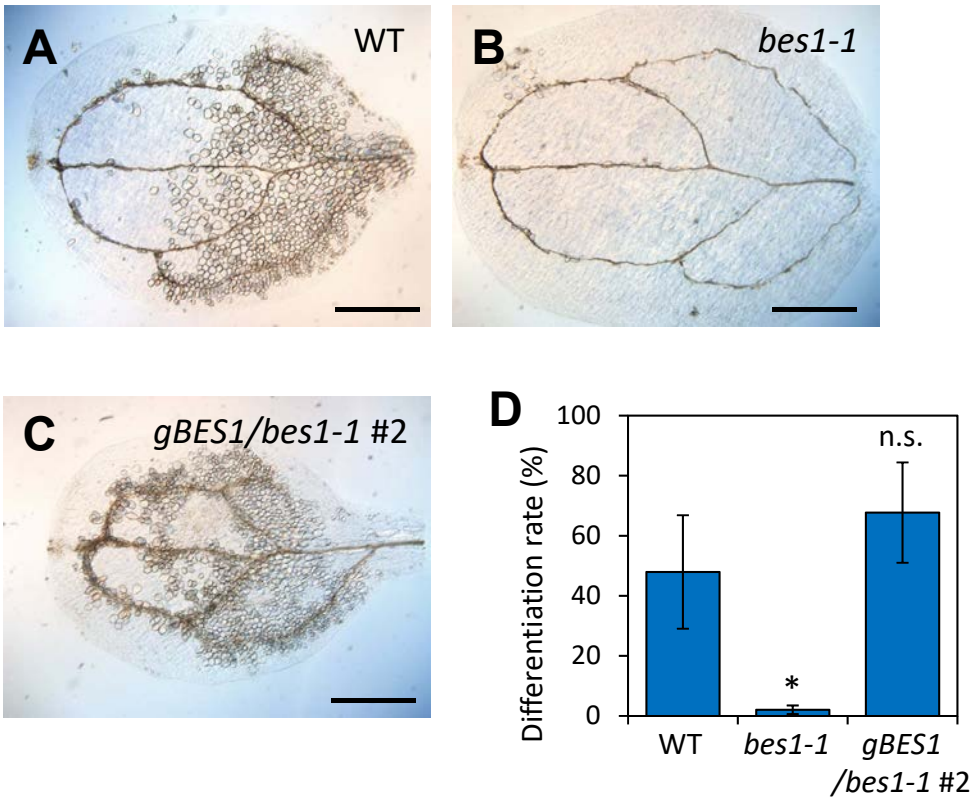

Figure 7. Complementation test.
(A-C) Ectopic xylem cell formation in VISUAL. Cotyledons of the WT (A), *bes1-1* (B), and *bes1-1* harboring genomic *BES1* (*gBES1/bes1-1*) (C) were cultured for 4 days. Scale bars indicate 1 mm. (D) Quantification of xylem differentiation rates in A-C. Error bars indicate SD (n = 8). Significant differences compared with the WT were examined by Tamhane T2 test ($\alpha = 0.05$).

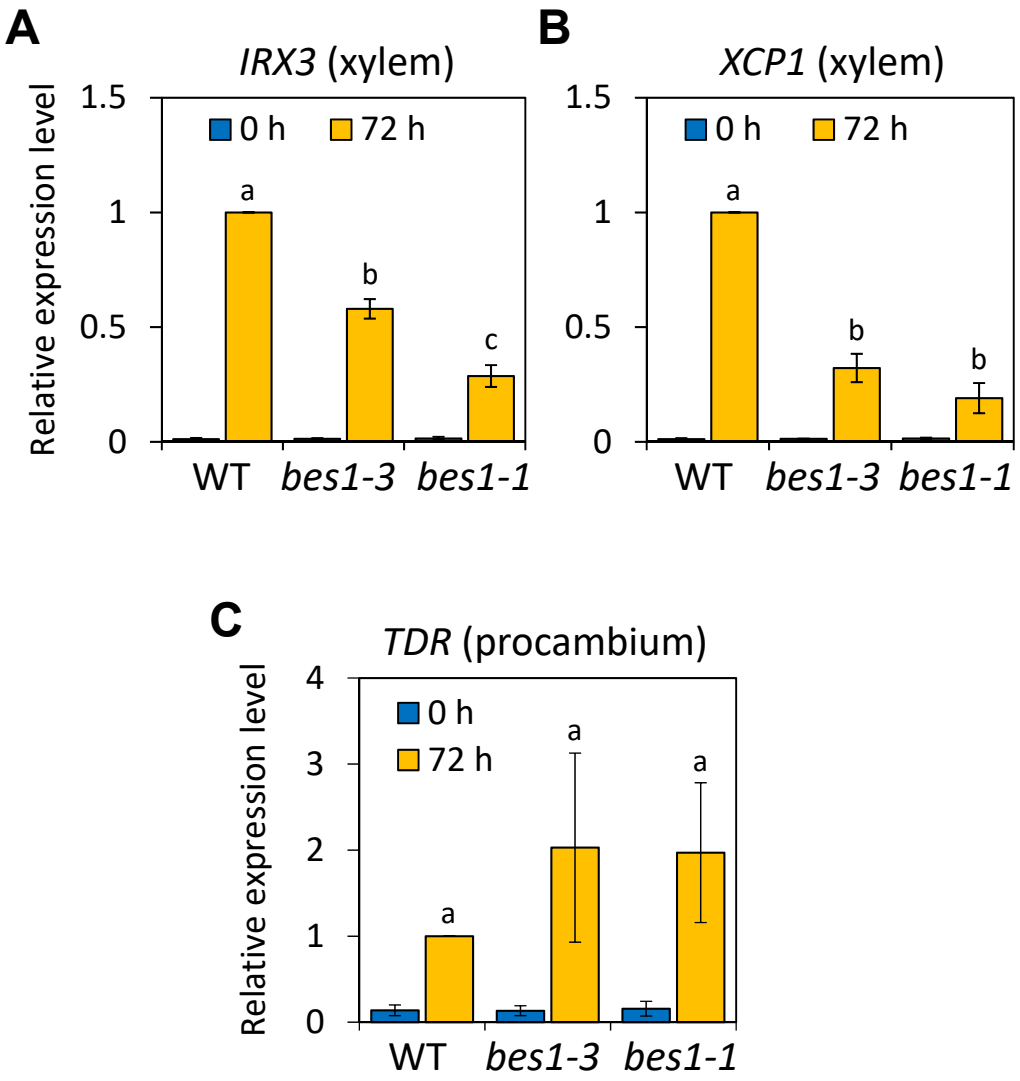

Figure 8. Gene expression analysis of *bes1* mutants in VISUAL.

(A-C) Expression levels of vascular-related marker genes in VISUAL. *IRX3* (A) and *XCP1* (B) are xylem-specific markers, *TDR* (C) is a procambium marker. Relative expression levels were calculated by comparison with gene expression levels at 72 h in the WT. Error bars indicate SD (n = 3). Significant differences among samples after induction are indicated by different letters (Tamhane T2 test, $\alpha = 0.05$).

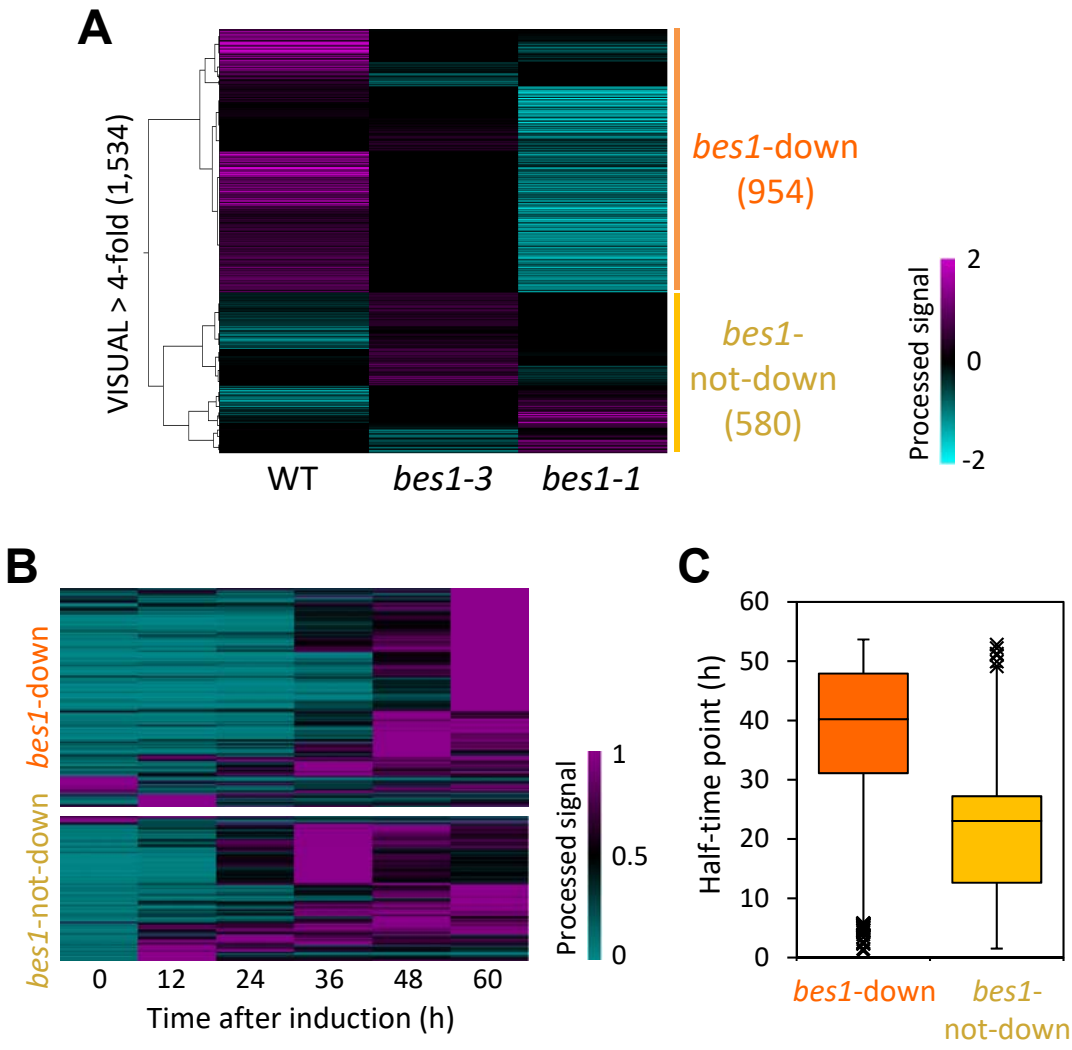

Figure 9. Microarray analysis of *bes1* mutants in VISUAL.

(A) Hierarchical clustering of vascular-related genes. Each gene expression level was normalized by setting the median value of the WT, *bes1-3*, and *bes1-1* as 0 (See Methods section). Two major clades were defined as the *bes1*-down and *bes1*-not-down group based on expression pattern. Relative gene expression levels are visualized in a heatmap image according to the color scale shown in the right panel. (B) Comparison of time-course of expression patterns between the *bes1*-down and *bes1*-not-down group. Each gene expression level was normalized by dividing the level by its maximum. (C) Box plot showing the distribution of the half-time point for each gene. The half-time point is defined as the first time point when the relative expression level reached 50% of its maximum. “x” symbols indicate outliers.

5年以内に雑誌で刊行予定のため、非公開

Figure 10.

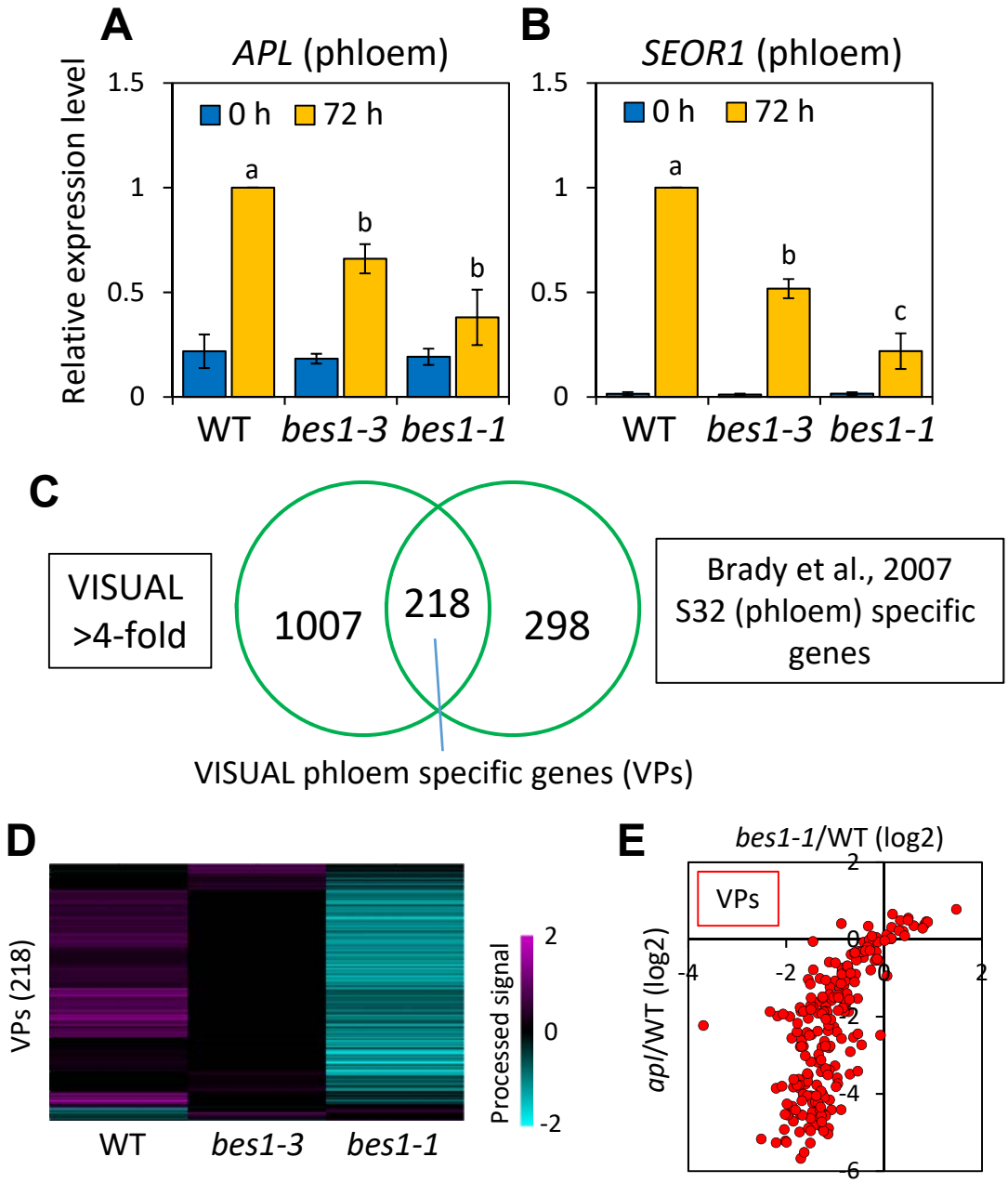

Figure 11. Phloem differentiation of *bes1* mutants in VISUAL.

(A,B) Expression levels of phloem marker genes *APL* (A) and *SEOR1* (B) in VISUAL. Relative expression levels were calculated by comparison with gene expression levels at 72 h in the WT. Error bars indicate SD (n = 3). Significant differences among samples after induction are indicated by different letters (Tamhane T2 test, $\alpha = 0.05$). (C) VISUAL phloem-specific genes (VPs, Kondo et al., 2016). (D) Comparison of the expression patterns of VPs. Expression levels are visualized in a heatmap image according to the color scale shown in the right panel. (E) Comparison of the expression patterns of VPs in the WT vs. *bes1-1* and the WT vs. *apl* (Kondo et al., 2016) in VISUAL. Horizontal axis and vertical axis represent fold-change in *bes1-1* and *apl* against the WT at log2 scale, respectively.

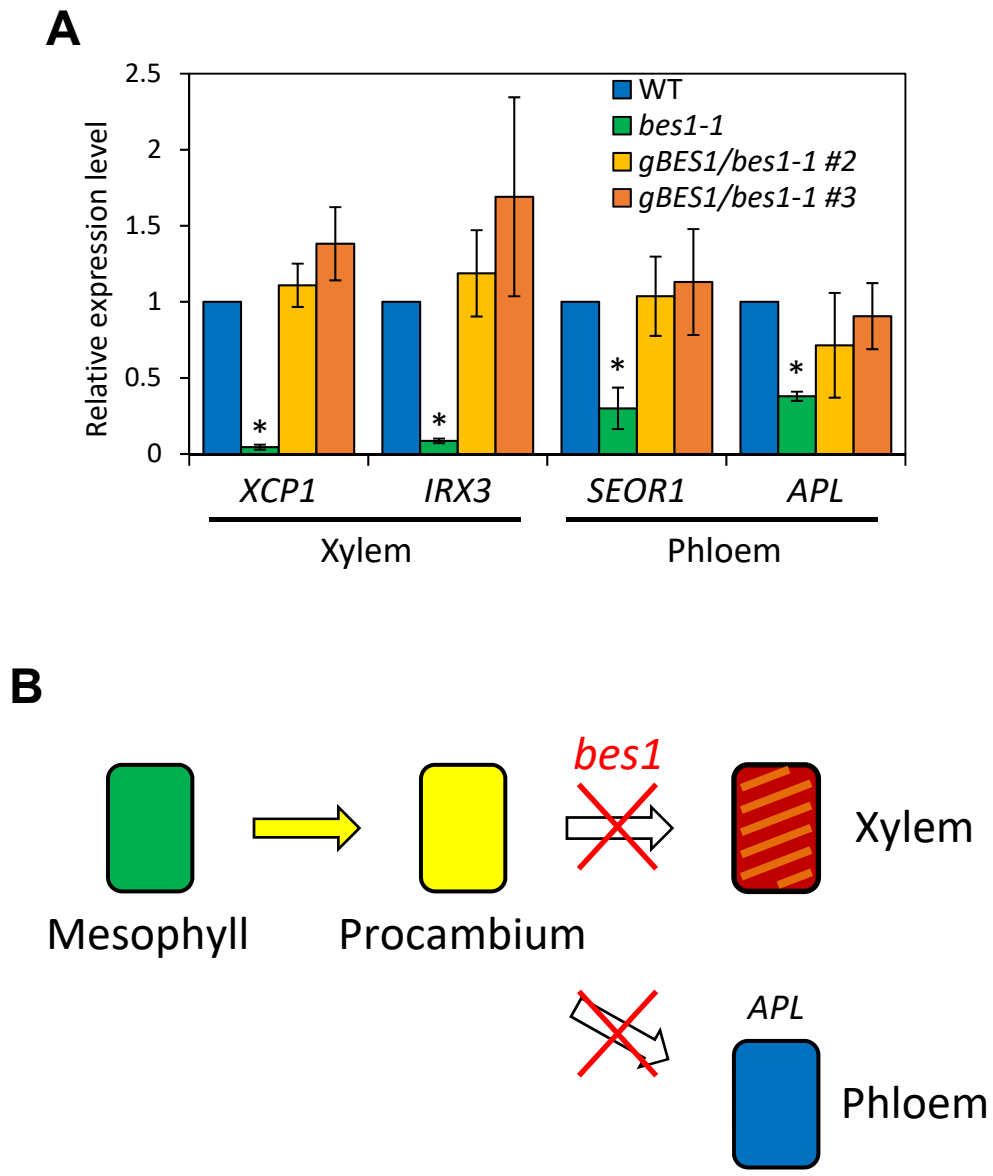

Figure 12. Summary of *bes1* mutant phenotypes in VISUAL

(A) Expression levels of xylem and phloem marker genes in VISUAL. RNA was extracted from cotyledons at 72 h after VISUAL induction. Two independent complement lines were examined. Relative expression levels were calculated by comparison with the WT. Error bars indicate SD (n = 3). Significant differences compared with the WT were examined by Tamhane T2 test ($\alpha = 0.05$). (B) Schematic illustration of the *bes1* mutant phenotype in VISUAL. The *bes1* mutations repress xylem and phloem differentiation from procambial cells. Procambial cells are formed even in *bes1* mutants.

5年以内に雑誌で刊行予定のため、非公開

Figure 13.

5年以内に雑誌で刊行予定のため、非公開

Figure 14.

5年以内に雑誌で刊行予定のため、非公開

Figure 15.

5年以内に雑誌で刊行予定のため、非公開

Figure 16.

5年以内に雑誌で刊行予定のため、非公開

Figure 17.

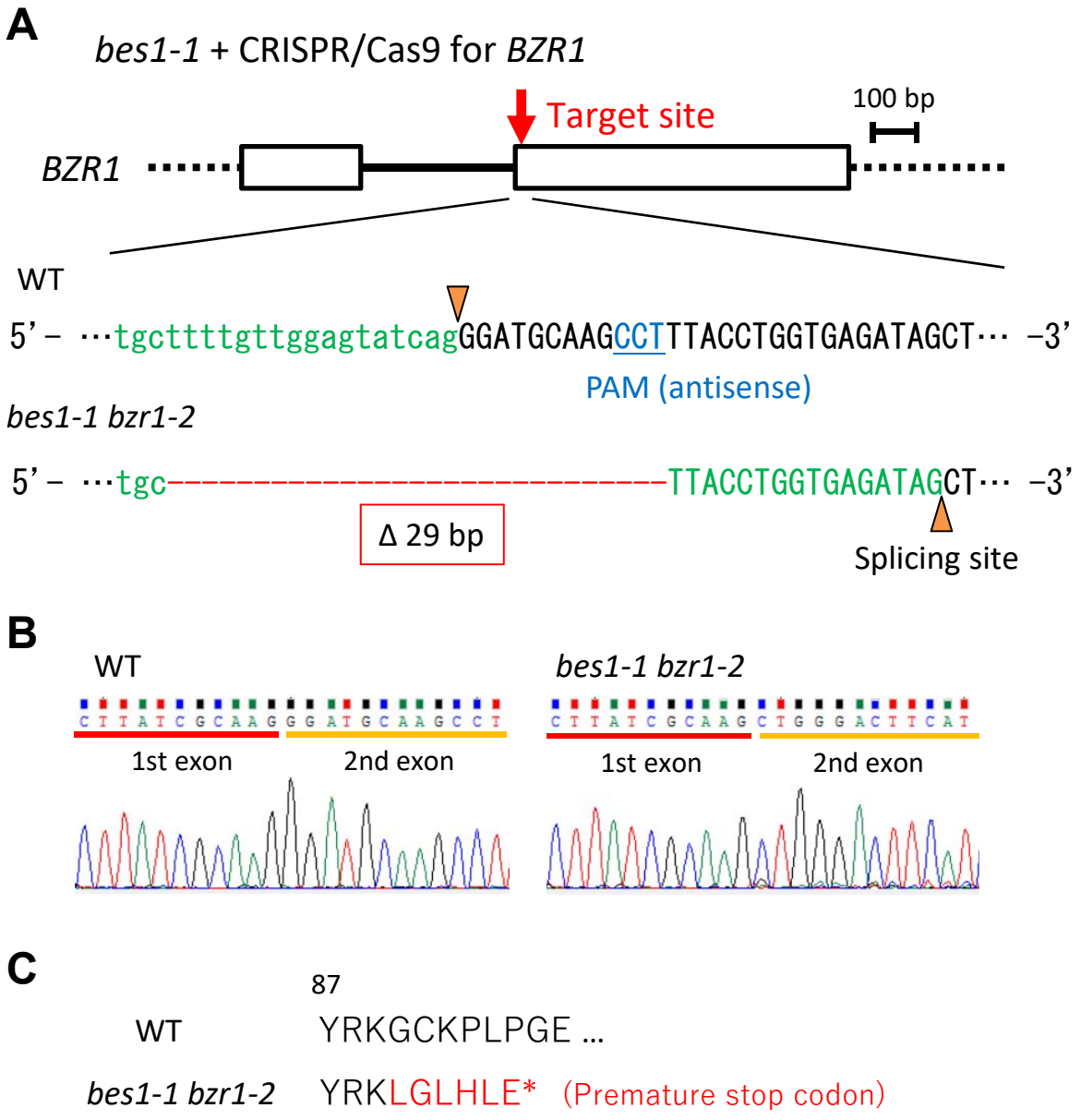

Figure 18. Generation of *bes1 bzr1* mutants.

(A) Schematic overview of the gene structure of *BZR1* and the sequence around the selected site targeted by CRISPR/Cas9. Exons, the intron, and UTRs are illustrated by boxes, a solid line, and dotted lines, respectively. Exon and intron sequences in the WT are shown in lowercase and uppercase letters, respectively. PAM sequences of the target and the resulting mutations are highlighted in blue and red, respectively. Twenty nine base deletions occurred in *bes1-1 bzr1-2*. (B) The mRNA sequences of *BZR1* in the WT and *bes1-1 bzr1-2*. The splicing site in each line is marked by an arrowhead, and spliced sequences are highlighted in green in A. (C) Theoretical amino acid sequences of BZR1 around the mutated sites in the WT and *bes1-1 bzr1-2*. Asterisk represents premature stop codons.

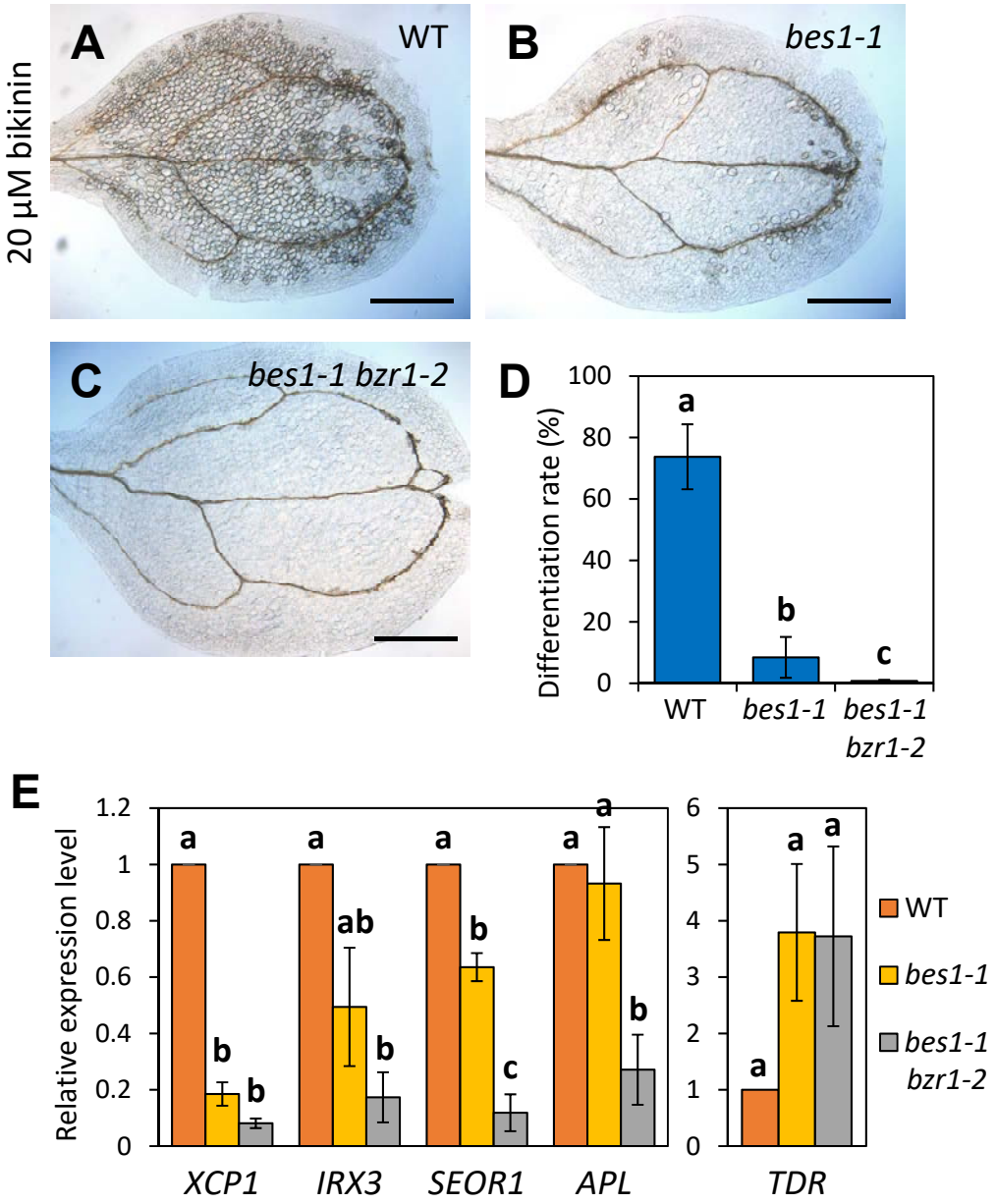

Figure 19. Mutant phenotypes of *bes1-1 bzr1-2* in VISUAL.

(A-C) Ectopic xylem cell formation in VISUAL. WT (A), *bes1-1* (B), and *bes1-1 bzr1-2* (C) cotyledons were cultured with bikinin at twice the normal concentration (20 μM) for 4 days. Scale bars indicate 1 mm. (D) Quantification of xylem differentiation rates in A-C. Error bars indicate SD (n = 8–12). Significant differences are indicated by different letters (Tamhane T2 test, $\alpha = 0.05$). (E) Expression levels of xylem, phloem, and procambium marker genes in the WT, *bes1-1*, and *bes1-1 bzr1-2* in VISUAL in the presence of 20 μM bikinin. RNA was extracted from cotyledons at 72 h after induction. Relative expression levels were calculated by comparison with the WT. Error bars indicate SD (n = 3). Significant differences are indicated by different letters (Tamhane T2 test, $\alpha = 0.05$).

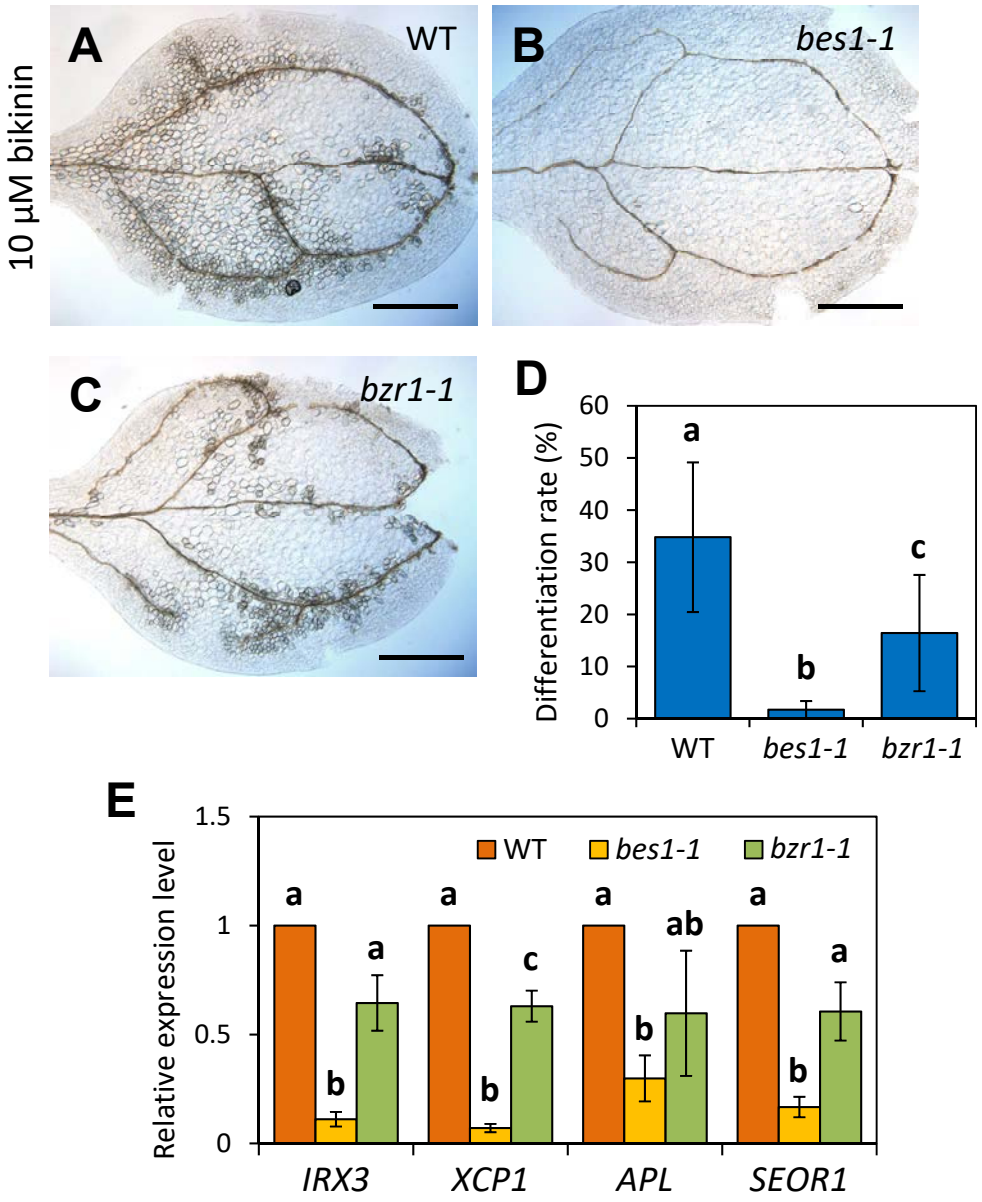

Figure 20. Mutant phenotypes of *bzr1* in VISUAL.

(A-C) Ectopic xylem cell formation in VISUAL. WT (A), *bes1-1* (B), and *bzr1* (C) cotyledons were cultured for 4 days. Scale bars indicate 1 mm. (D) Quantification of xylem differentiation rates in A-C. Error bars indicate SD (n = 8). Significant differences are indicated by different letters (Tamhane T2 test, α = 0.05). (E) Expression levels of xylem and phloem marker genes in the WT, *bes1-1*, and *bzr1* in VISUAL. RNA was extracted from cotyledons at 72 h after VISUAL induction. Relative expression levels were calculated by comparison with the WT. Error bars indicate SD (n = 3). Significant differences are indicated by different letters (Tamhane T2 test, α = 0.05).

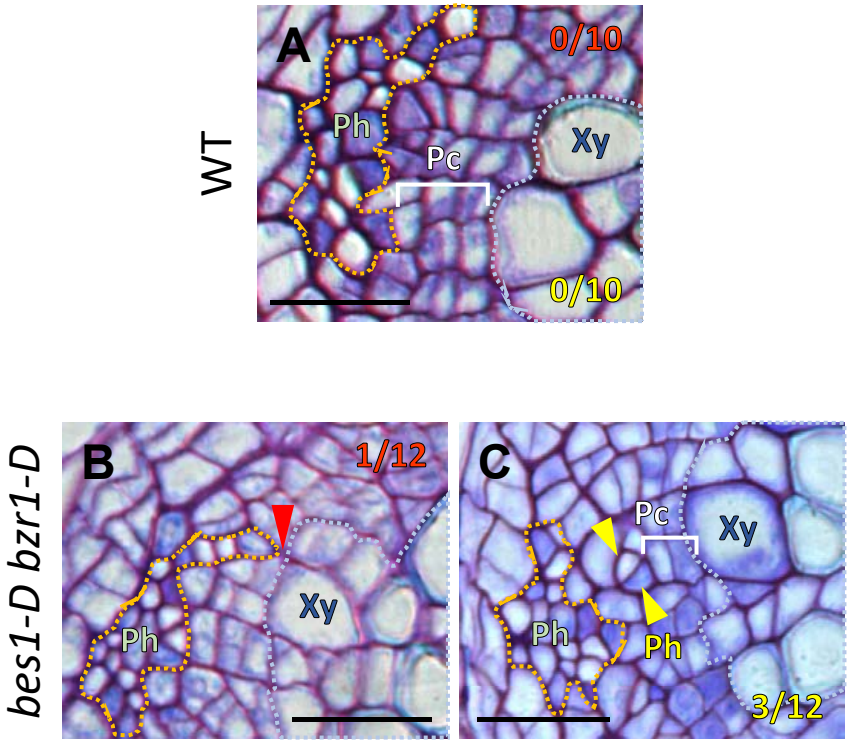

Figure 21. Comparison of hypocotyl vasculature between WT and *bes1-D bzr1-D*.

Cross-sections of hypocotyls of WT (A) and *bes1-D bzr1-D* (B, C) plants grown for 11 days. Orange and blue dotted lines indicate phloem (Ph) and xylem (Xy) cells, respectively. White solid lines indicate procambial cell (Pc) layers. Pairs of phloem sieve element and companion cell were distinguished by thin and dense staining of toluidine blue. Red and yellow arrowheads indicate the adjacency of xylem and phloem cells and non-clustered phloem cells, respectively. Fraction in the upper and lower of each picture represent the number of plants exhibiting adjacency of xylem and phloem cells and non-clustered phloem cells per total number of plants observed, respectively. Scale bars indicate 20 μm.

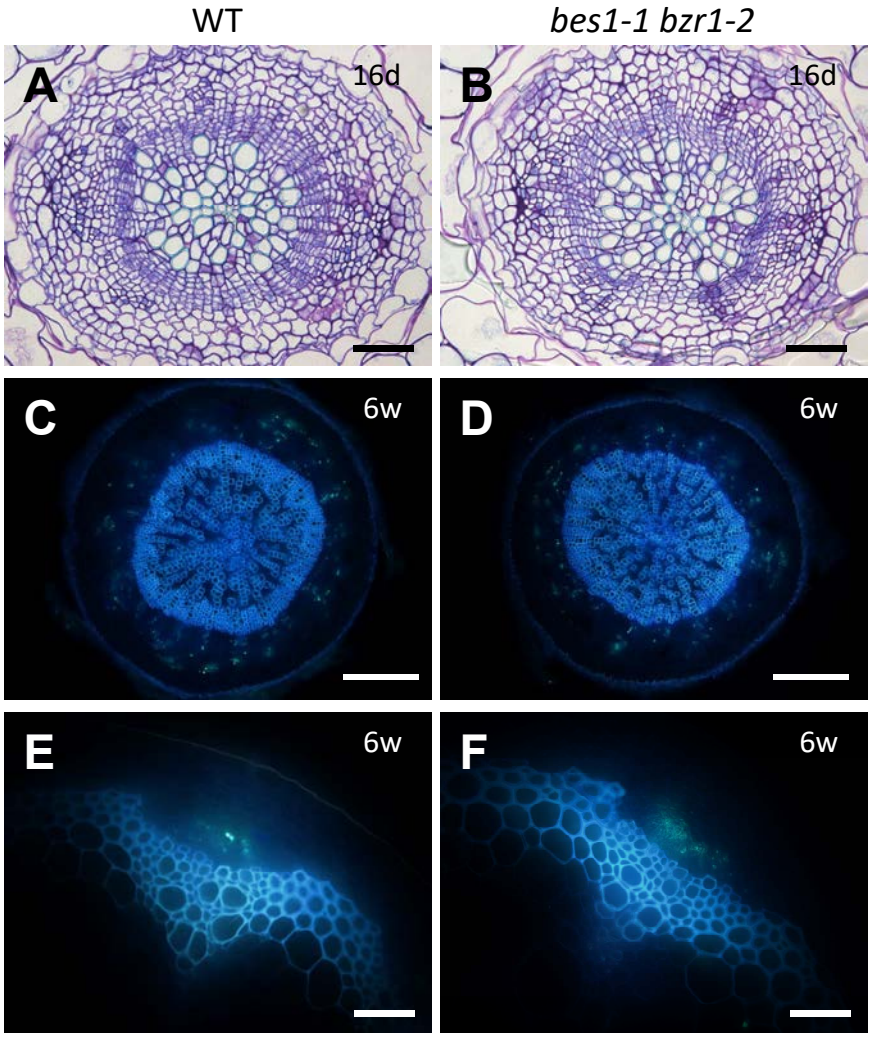

Figure 22. *In vivo* vascular formation of *bes1-1 bzr1-2*.

(A-F) Cross-sections of hypocotyls (A-D) and stems (E, F) of WT (A, C, E) and *bes1-1 bzr1-2* (B, D, F) plants grown for 16 days (A, B) or 6 weeks (C-F). Toluidine blue (A, B) or aniline blue staining (C-F) was conducted. Blue and green fluorescence in C-F is autofluorescence from xylem cells and stained phloem cells after UV radiation, respectively. Scale bars indicate 200 μm for C-D and 50 μm for the others.

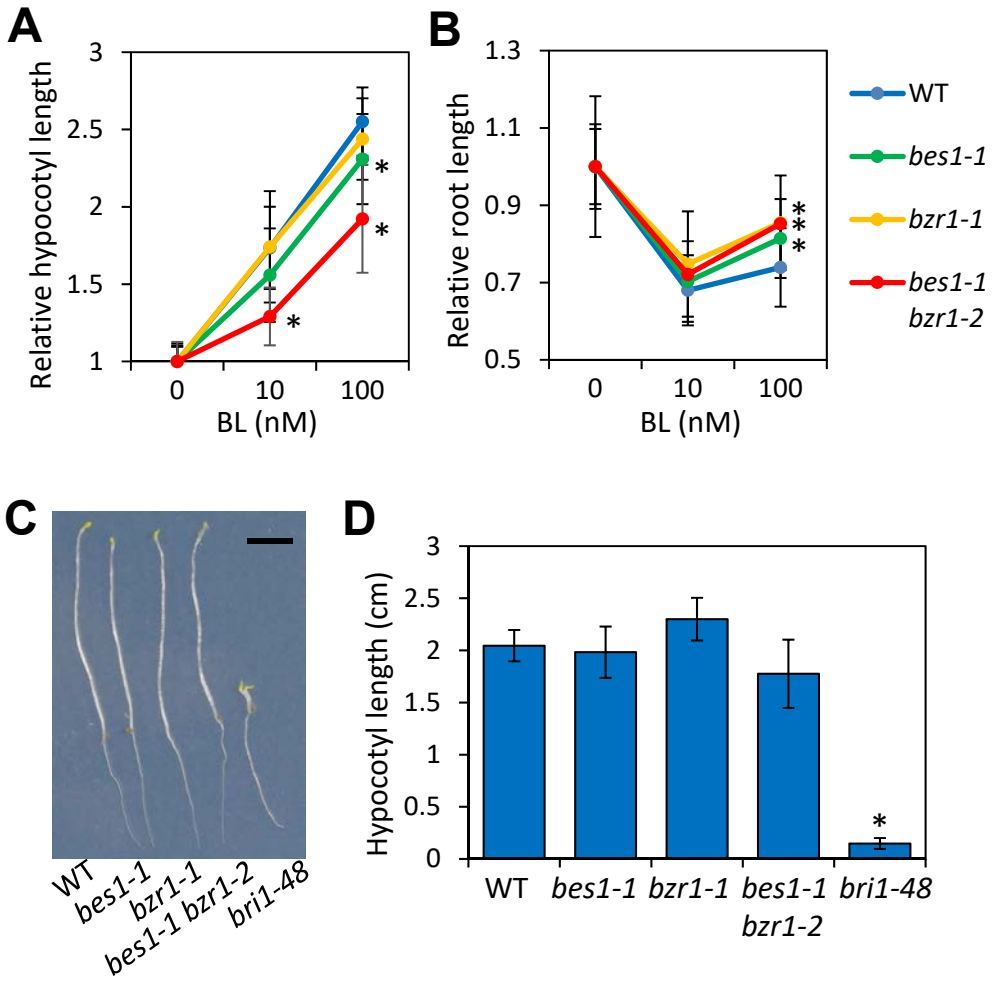

Figure 23. *In vivo* BR-related phenotypes of *bes1-1 bzr1-2*.

(A, B) BL sensitivity of WT, *bes1-1*, *bzr1-1* and *bes1-1 bzr1-2* seedlings. Relative lengths of hypocotyls (A) and roots (B) were calculated by comparison with samples of each genotype grown without BL. Error bars indicate SD (n = 30–32 except for n = 25 for *bzr1-1* treated with 10 nM BL). (C) Hypocotyl elongation in plants grown in the dark. Seedlings were grown for 7 days. The scale bar indicates 0.5 cm. (D) Quantification of hypocotyl elongation in I. Error bars indicate SD (n = 3–6). Significant differences compared with the WT were examined by Tamhane T2 test (α = 0.05).

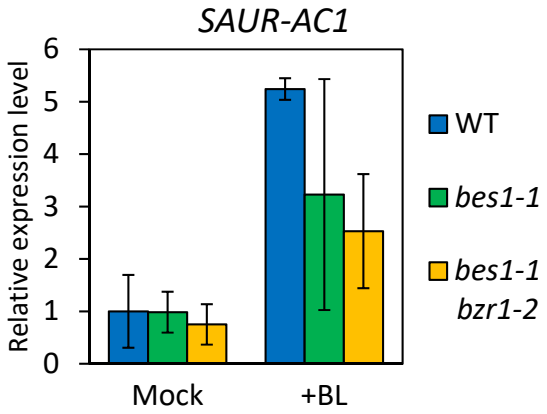

Figure 24. BR-responsive gene expression in *bes1-1 bzr1-2*.

Expression levels of *SAUR-AC1* in 10-day-old WT, *bes1-1* and *bes1-1 bzr1-2* treated with 100 nM BL or mock for 3 hours. Relative expression levels were calculated by comparison with those of the WT under mock treatment. Error bars indicate SD (n = 3).

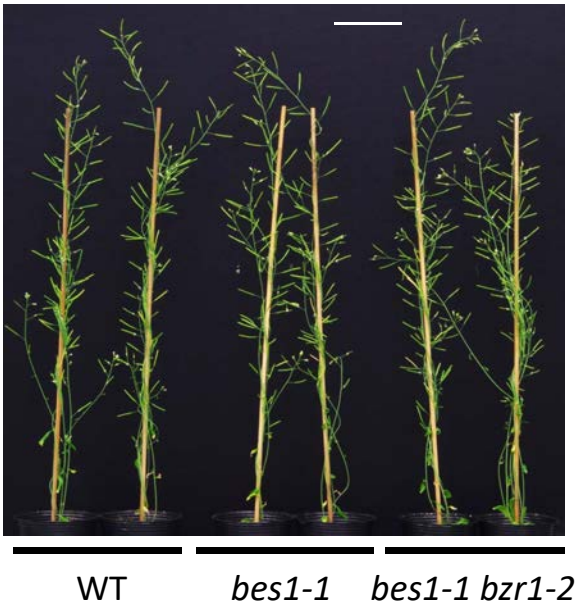

Figure 25. Growth phenotype of *bes1-1 bzr1-2*.

Stems of 40-day-old WT, *bes1-1* and *bes1-1 bzr1-2*. The scale bar indicates 5 cm.

5年以内に雑誌で刊行予定のため、非公開

Figure 26.

5年以内に雑誌で刊行予定のため、非公開

Figure 27.

5年以内に雑誌で刊行予定のため、非公開

Figure 28.

5年以内に雑誌で刊行予定のため、非公開

Figure 29.

References

Anne, P., Azzopardi, M., Gissot, L., Beaubiat, S., Hématy, K. and Palauqui, J.C. (2015) OCTOPUS Negatively Regulates BIN2 to Control Phloem Differentiation in *Arabidopsis thaliana*. *Curr*. *Biol*. 25: 2584–2590.

Bai, M.Y., Zhang, L.Y., Gampala, S.S., Zhu, S.W., Song, W.Y., Chong, K. and Wang, Z.Y. (2007) Functions of OsBZR1 and 14-3-3 proteins in brassinosteroid signaling in rice. *Proc*. *Natl*. *Acad*. *Sci*. *USA* 104: 13839–13844.

Bonke, M., Thitamadee, S., Mähönen, A.P., Hauser, M.T. and Helariutta, Y. (2003) APL regulates vascular tissue identity in *Arabidopsis*. *Nature* 426: 181–186.

Brady, S.M., Orlando, D.A., Lee, J.Y., Wang, J.Y., Koch, J., Dinneny, J.R., Mace, D., Ohler, U. and Benfey, P.N. (2007) A high-resolution root spatiotemporal map reveals dominant expression patterns. *Science* 318: 801–806.

Cheng, Y., Zhu, W., Chen, Y., Ito, S., Asami, T. and Wang, X. (2014) Brassinosteroids control root epidermal cell fate via direct regulation of a MYB-bHLH-WD40 complex by GSK3-like kinases. *eLife* 3: e02525.

Cho, H., Ryu, H., Rho, S., Hill, K., Smith, S., Audenaert, D., Park, J., Han, S., Beeckman, T., Bennett, M.J., Hwang, D., De Smet, I. and Hwang, I. (2014) A secreted peptide acts on BIN2-mediated phosphorylation of ARFs to potentiate auxin response

during lateral root development. *Nat. Cell Biol*. 16: 66–76.

Clough, S.J. and Bent, A.F. (1998) Floral dip: a simplified method for *Agrobacterium*-mediated transformation of *Arabidopsis thaliana*. *Plant J*. 16: 735–743.

De Rybel, B., Audenaert, D., Vert, G., Rozhon, W., Mayerhofer, J., Peelman, F., Coutuer, S., Denayer, T., Jansen, L., Nguyen, L., Vanhoutte, I., Beemster, G.T., Vleminckx, K., Jonak, C., Chory, J., Inzé, D., Russinova, E. and Beeckman, T. (2009) Chemical inhibition of a subset of *Arabidopsis thaliana* GSK3-like kinases activates brassinosteroid signaling. *Chem*. *Biol*. 16: 594–604.

Endo, H., Yamaguchi, M., Tamura, T., Nakano, Y., Nishikubo, N., Yoneda, A., Kato, K., Kubo, M., Kajita, S., Katayama, Y., Ohtani, M. and Demura, T. (2015) Multiple classes of transcription factors regulate the expression of VASCULAR-RELATED NAC-DOMAIN7, a master switch of xylem vessel differentiation. *Plant Cell Physiol*. 56: 242–254.

Endo, M., Shimizu, H., Nohales, M.A., Araki, T. and Kay, S.A. (2014) Tissue-specific clocks in *Arabidopsis* show asymmetric coupling. *Nature* 515: 419–422.

Espinosa-Ruiz, A., Martínez, C., de Lucas, M., Fàbregas, N., Bosch, N., Caño-Delgado, A.I. and Prat, S. (2017) TOPLESS mediates brassinosteroid control of shoot boundaries and root meristem development in *Arabidopsis thaliana*. *Development* 144: 1619–1628.

Fauser, F., Schiml, S. and Puchta, H. (2014) Both CRISPR/Cas-based nucleases and nickases can be used efficiently for genome engineering in *Arabidopsis thaliana*. *Plant J*. 79: 348–359.

Furuta, K.M., Hellmann, E. and Helariutta, Y. (2014a) Molecular control of cell specification and cell differentiation during procambial development. *Annu*. *Rev*. *Plant Biol*. 65: 607–638.

Furuta, K.M., Yadav, S.R., Lehesranta, S., Belevich, I., Miyashima, S., Heo, J.O., Vatén, A., Lindgren, O., De Rybel, B., Van Isterdael, G., Somervuo, P., Lichtenberger, R., Rocha, R., Thitamadee, S., Tähtiharju, S., Auvinen, P., Beeckman, T., Jokitalo, E. and Helariutta, Y. (2014b) *Arabidopsis* NAC45/86 direct sieve element morphogenesis culminating in enucleation. *Science* 345: 933–937.

Gampala, S.S., Kim, T.W., He, J.X., Tang, W., Deng, Z., Bai, M.Y., Guan, S., Lalonde, S., Sun, Y., Gendron, J.M., Chen, H., Shibagaki, N., Ferl, R.J., Ehrhardt, D., Chong, K., Burlingame, A.L. and Wang, Z.Y. (2007) An essential role for 14-3-3 proteins in brassinosteroid signal transduction in Arabidopsis. *Dev*. *Cell* 13:177–189.

Guo, H., Li, L., Aluru, M. and Yin, Y. (2013) Mechanisms and networks for brassinosteroid regulated gene expression. *Curr*. *Opin*. *Plant Biol*. 16: 545–553.

He, J.X., Gendron, J.M., Sun, Y., Gampala, S.S., Gendron, N., Sun, C.Q. and Wang, Z.Y. (2005) BZR1 is a transcriptional repressor with dual roles in brassinosteroid

homeostasis and growth responses. *Science* 307: 1634–1638.

He, J.X., Gendron, J.M., Yang, Y., Li, J. and Wang, Z.Y. (2002) The GSK3-like kinase BIN2 phosphorylates and destabilizes BZR1, a positive regulator of the brassinosteroid signaling pathway in *Arabidopsis*. *Proc*. *Natl*. *Acad*. *Sci*. *USA* 99: 10185–10190.

Hirakawa, Y., Shinohara, H., Kondo, Y., Inoue, A., Nakanomyo, I., Ogawa, M., Sawa, S., Ohashi-Ito, K., Matsubayashi, Y. and Fukuda, H. (2008) Non-cell-autonomous control of vascular stem cell fate by a CLE peptide/receptor system. *Proc*. *Natl*. *Acad*. *Sci*. *USA* 105: 15208–15213.

Hiratsu, K., Matsui, K., Koyama, T. and Ohme-Takagi, M. (2003) Dominant repression of target genes by chimeric repressors that include the EAR motif, a repression domain, in *Arabidopsis*. *Plant J*. 34: 733–739.

Huang, D.W., Sherman, B.T. and Lempicki, R.A. (2009) Systematic and integrative analysis of large gene lists using DAVID Bioinformatics Resources. *Nature Protoc*. 4: 44–57.

Ito, Y., Nakanomyo, I., Motose, H., Iwamoto, K., Sawa, S., Dohmae, N. and Fukuda, H. (2006) Dodeca-CLE peptides as suppressors of plant stem cell differentiation. *Science* 313: 842–845.

Jiang, J., Zhang, C. and Wang, X. (2015) A recently evolved isoform of the transcription

factor BES1 promotes brassinosteroid signaling and development in *Arabidopsis thaliana*. *Plant Cell* 27: 361–374.

Kagale, S., Links, M.G. and Rozwadowski, K. (2010) Genome-wide analysis of ethylene-responsive element binding factor-associated amphiphilic repression motif-containing transcriptional regulators in Arabidopsis. *Plant Physiol.* 152: 1109–1134.

Kang, S., Yang, F., Li, L., Chen, H., Chen, S. and Zhang, J. (2015) The Arabidopsis transcription factor BRASSINOSTEROID INSENSITIVE1-ETHYL METHANESULFONATE-SUPPRESSOR1 is a direct substrate of MITOGEN-ACTIVATED PROTEIN KINASE6 and regulates immunity. *Plant Physiol.* 167: 1076–1086.

Kondo, Y., Fujita, T., Sugiyama, M. and Fukuda, H. (2015) A novel system for xylem cell differentiation in *Arabidopsis thaliana*. *Mol. Plant* 8: 612–621.

Kondo, Y., Ito, T., Nakagami, H., Hirakawa, Y., Saito, M., Tamaki, T., Shirasu, K. and Fukuda, H. (2014) Plant GSK3 proteins regulate xylem cell differentiation downstream of TDIF-TDR signalling. *Nat. Commun*. 5: 3504.

Kondo, Y., Nurani, A.M., Saito, C., Ichihashi, Y., Saito, M., Yamazaki, K., Mitsuda, N., Ohme-Takagi, M. and Fukuda, H. (2016) Vascular Cell Induction Culture System Using Arabidopsis Leaves (VISUAL) reveals the sequential differentiation of sieve

element-like cells. *Plant Cell* 28: 1250–1262.

Kubo, M., Udagawa, M., Nishikubo, N., Horiguchi, G., Yamaguchi, M., Ito, J., Mimura, T., Fukuda, H. and Demura, T. (2005) Transcription switches for protoxylem and metaxylem vessel formation. *Genes Dev*. 19: 1855–1860.

Lachowiec, J., Lemus, T., Thomas, J.H., Murphy, P.J., Nemhauser, J.L. and Queitsch, C. (2013) The protein chaperone HSP90 can facilitate the divergence of gene duplicates. *Genetics* 193: 1269–1277.

Li, J. and Chory, J. (1997) A putative leucine-rich repeat receptor kinase involved in brassinosteroid signal transduction. *Cell* 90: 929–938.

Li, J. and Nam, K.H. (2002) Regulation of brassinosteroid signaling by a GSK3/SHAGGY-like kinase. *Science* 295: 1299–1301.

Naito, Y., Hino, K., Bono, H. and Ui-Tei, K. (2015) CRISPRdirect: software for designing CRISPR/Cas guide RNA with reduced off-target sites. *Bioinformatics* 31: 1120–1123.

Nakagawa, T., Kurose, T., Hino, T., Tanaka, K., Kawamukai, M., Niwa, Y., Toyooka, K., Matsuoka, K., Jinbo, T. and Kimura, T. (2007) Development of series of gateway binary vectors, pGWBs, for realizing efficient construction of fusion genes for plant transformation. *J. Biosci. Bioeng*. 104: 34–41.

Oh, E., Zhu, J.Y., Ryu, H., Hwang, I. and Wang, Z.Y. (2014) TOPLESS mediates brassinosteroid-induced transcriptional repression through interaction with BZR1. *Nat*. *Commun*. 5: 4140.

Ohashi-Ito, K., Oda, Y. and Fukuda, H. (2010) *Arabidopsis* VASCULAR-RELATED NAC-DOMAIN6 directly regulates the genes that govern programmed cell death and secondary wall formation during xylem differentiation. *Plant Cell* 22: 3461–3473.

Rodriguez-Villalon, A., Gujas, B., van Wijk, R., Munnik, T. and Hardtke, C.S. (2015) Primary root protophloem differentiation requires balanced phosphatidylinositol-4,5-biphosphate levels and systemically affects root branching. *Development* 142: 1437–1446.

Rozhon, W., Mayerhofer, J., Petutschnig, E., Fujioka, S. and Jonak, C. (2010) ASKtheta, a group-III Arabidopsis GSK3, functions in the brassinosteroid signalling pathway. *Plant J*. 62: 215–223.

Ryu, H., Cho, H., Bae, W. and Hwang, I. (2013) Control of early seedling development by BES1/TPL/HDA19-mediated epigenetic regulation of ABI3. *Nat*. *Commun*. 5: 4138.

Ryu, H., Cho, H., Kim, K. and Hwang, I. (2010) Phosphorylation dependent nucleocytoplasmic shuttling of BES1 is a key regulatory event in brassinosteroid signaling. *Mol*. *Cells* 29: 283–290.

Ryu, H., Kim, K., Cho, H., Park, J., Choe, S. and Hwang, I. (2007) Nucleocytoplasmic shuttling of BZR1 mediated by phosphorylation is essential in *Arabidopsis* brassinosteroid signaling. *Plant Cell*, 19: 2749–2762.

Sawchuk, M.G., Donner, T.J., Head, P. and Scarpella, E. (2008) Unique and overlapping expression patterns among members of photosynthesis-associated nuclear gene families in Arabidopsis. *Plant Physiol*. 148: 1908–1924.

Singh, M.B. and Bhalla, P.L. (2006) Plant stem cells carve their own niche. *Trends Plant Sci.* 11: 241–246.

Soyano, T., Thitamadee, S., Machida, Y. and Chua, N.H. (2008) ASYMMETRIC LEAVES2-LIKE19/LATERAL ORGAN BOUNDARIES DOMAIN30 and ASL20/LBD18 regulate tracheary element differentiation in *Arabidopsis*. *Plant Cell* 20: 3359–3373.

Sun, Y., Fan, X.Y., Cao, D.M., Tang, W., He, K., Zhu, J.Y., He, J.X., Bai, M.Y., Zhu, S., Oh, E., Patil, S., Kim, T.W., Ji, H., Wong, W.H., Rhee, S.Y. and Wang, Z.Y. (2010) Integration of brassinosteroid signal transduction with the transcription network for plant growth regulation in *Arabidopsis*. *Dev. Cell* 19: 765–777.

Sundell, D., Street, N.R., Kumar, M., Mellerowicz, E.J., Kucukoglu, M., Johnsson, C., Kumar, V., Mannapperuma, C., Delhomme, N., Nilsson, O., Tuominen, H., Pesquet, E.,

Fischer, U., Niittylä, T., Sundberg, B. and Hvidsten, T.R. (2017) AspWood: high-spatial-resolution transcriptome profiles reveal uncharacterized modularity of wood formation in *Populus tremula*. *Plant Cell* 29: 1585–1604.

Tan, T.T., Endo, H., Sano, R., Kurata, T., Yamaguchi, M., Ohtani, M. and Demura, T. (2018) Transcription factors VND1-VND3 contribute to cotyledon xylem vessel formation. *Plant Physiol*. 176: 773–789.

Tang, W., Deng, Z., Oses-Prieto, J.A., Suzuki, N., Zhu, S., Zhang, X., Burlingame, A.L. and Wang, Z.Y. (2008) Proteomics studies of brassinosteroid signal transduction using prefractionation and two-dimensional DIGE. *Mol*. *Cell Proteomics* 7: 728–738.

Unterholzner, S.J., Rozhon, W., Papacek, M., Ciomas, J., Lange, T., Kugler, K.G., Mayer, K.F., Sieberer, T. and Poppenberger, B. (2015) Brassinosteroids are master regulators of gibberellin biosynthesis in *Arabidopsis*. *Plant Cell* 27: 2261–2272.

Verhoef, N., Yokota, T., Shibata, K., de Boer, G.J., Gerats, T., Vandenbussche, M., Koes, R. and Souer, E. (2013) Brassinosteroid biosynthesis and signalling in *Petunia hybrida*. *J*. *Exp*. *Bot*. 64: 2435–2448.

Vilarrasa-Blasi, J., González-García, M.P., Frigola, D., Fàbregas, N., Alexiou, K.G., López-Bigas, N., Rivas, S., Jauneau, A., Lohmann, J.U., Benfey, P.N., Ibañes, M., Caño-Delgado, A.I. (2014) Regulation of plant stem cell quiescence by a brassinosteroid signaling module. *Dev Cell*. 30: 36–47.

Wallner, E.S., López-Salmerón, V., Belevich, I., Poschet, G., Jung, I. and Grünwald, K., Sevilem, I., Jokitalo, E., Hell, R., Helariutta, Y., Agustí, J., Lebovka, I. and Greb, T. (2017) Strigolactone- and karrikin-independent SMXL proteins are central regulators of phloem formation. *Curr*. *Biol*. 27: 1241–1247.

Wang, Y., Sun, S., Zhu, W., Jia, K., Yang, H. and Wang, X. (2013) Strigolactone/MAX2-induced degradation of brassinosteroid transcriptional effector BES1 regulates shoot branching. *Dev*. *Cell* 27: 681–688.

Wang, Z.Y., Nakano, T., Gendron, J., He, J., Chen, M., Vafeados, D., Yang, Y., Fujioka, S., Yoshida, S., Asami, T. and Chory, J. (2002) Nuclear-localized BZR1 mediates brassinosteroid-induced growth and feedback suppression of brassinosteroid biosynthesis. *Dev*. *Cell* 2: 505–513.

Yamaguchi, M., Mitsuda, N., Ohtani, M., Ohme-Takagi, M., Kato, K. and Demura, T. (2011) VASCULAR-RELATED NAC-DOMAIN7 directly regulates the expression of a broad range of genes for xylem vessel formation. *Plant J*. 66: 579–590.

Yang, M., Li, C., Cai, Z., Hu, Y., Nolan, T., Yu, F., Yin, Y., Xie, Q., Tang, G. and Wang, X. (2017) SINAT E3 ligases control the light-mediated stability of the brassinosteroid-activated transcription factor BES1 in *Arabidopsis*. *Dev*. *Cell* 41: 47–58.

Yin, Y., Vafeados, D., Tao, Y., Yoshida, S., Asami, T. and Chory, J. (2005) A new class

of transcription factors mediates brassinosteroid-regulated gene expression in *Arabidopsis*. *Cell* 120: 249–259.

Yin, Y., Wang, Z.Y., Mora-Garcia, S., Li, J., Yoshida, S., Asami, T. and Chory, J. (2002) BES1 accumulates in the nucleus in response to brassinosteroids to regulate gene expression and promote stem elongation. *Cell* 109: 181–191.

Yokoyama, A., Yamashino, T., Amano, Y., Tajima, Y., Imamura, A., Sakakibara, H. and Mizuno, T. (2007) Type-B ARR transcription factors, ARR10 and ARR12, are implicated in cytokinin-mediated regulation of protoxylem differentiation in roots of *Arabidopsis thaliana*. *Plant Cell Physiol*. 48: 84–96.

Yu, X., Li, L., Zola, J., Aluru, M., Ye, H., Foudree, A., Guo, H., Anderson, S., Aluru, S., Liu, P., Rodermel, S. and Yin, Y. (2011) A brassinosteroid transcriptional network revealed by genome-wide identification of BES1 target genes in *Arabidopsis thaliana*. *Plant J*. 65: 634–646.

Zhang, Y., Zhang, Y.J., Yang, B.J., Yu, X.X., Wang, D., Zu, S.H., Xue, H.W. and Lin, W.H. (2016) Functional characterization of *GmBZL2* (*AtBZR1* like gene) reveals the conserved BR signaling regulation in *Glycine max*. *Sci*. *Rep*. 6: 31134.

Zhou, J., Zhong, R. and Ye, Z.H. (2014) Arabidopsis NAC domain proteins, VND1 to VND5, are transcriptional regulators of secondary wall biosynthesis in vessels. *PLoS One* 22: e105726.